A siliceous microfossil view of middle Eocene Arctic paleoenvironments: A window of biosilica production and preservation

Catherine E. Stickley,[1] Nalân Koç,[1,2] Hans-Jürgen Brumsack,[3] Richard W. Jordan,[4] and Itsuki Suto[5]

Received 30 April 2007; revised 3 October 2007; accepted 17 October 2007; published 13 March 2008.

[1] Integrated Ocean Drilling Program (IODP) Expedition 302, "The Arctic Coring Expedition" (ACEX), unearthed the most significant find of Paleogene siliceous microfossils in nearly 2 decades. 100 m of early middle Eocene, organic-rich, finely laminated sediments contain abundant marine and freshwater siliceous microfossils allowing intriguing insights into central Arctic paleoenvironments during the start of Cenozoic cooling. Largely endemic assemblages of marine diatoms and ebridians are preserved along with very high abundances of chrysophyte cysts, the endogenously formed resting stage of freshwater algae. An overall brackish environment is invoked, but variations in group dominance suggest episodic changes in salinity, stratification, and trophic status. With the backing of inorganic geochemistry we synthesize the sediment characteristics by hypothesizing an environmental model for the cooccurrence of these diverse siliceous microfossil groups. We also report on initial insights into the composition of some of the laminations, which may help explain the formation of this rich sediment archive.

Citation: Stickley, C. E., N. Koç, H.-J. Brumsack, R. W. Jordan, and I. Suto (2008), A siliceous microfossil view of middle Eocene Arctic paleoenvironments: A window of biosilica production and preservation, *Paleoceanography*, *23*, PA1S14, doi:10.1029/2007PA001485.

1. Introduction

[2] Until recently, information on central Arctic pre-Quaternary siliceous microfossils had been limited to a few short piston cores from the Alpha Ridge (AR; Figure 1), i.e., the USGS cores FL-437 (Late Cretaceous) and FL-422 (middle Eocene) [*Dell'Agnese and Clark*, 1994; *Bukry*, 1984] and the Canadian CESAR 6 core (Late Cretaceous) [*Barron*, 1985; *Bukry*, 1985]. Recently, *Davies* [2006] described diatom seasonality in laminations of the Late Cretaceous CESAR 6 core, yet such detailed information on the central Arctic Eocene deposits is undocumented.

[3] Eocene diatoms in sites proximal to the central Arctic are somewhat better known but records are still relatively patchy. Information exists from sites in the Norwegian and Greenland seas (Figure 1), e.g., DSDP Leg 38, Sites 338–340 and 343 [e.g., *Schrader and Fenner*, 1976; *Dzinoridze et al.*, 1978; *Fenner*, 1985] and ODP Leg 151, Site 913B [*Scherer and Koç*, 1996]; Danish outcrops, e.g., the Für Formation [*Homann*, 1991; *Fenner*, 1994] and Californian outcrops, e.g., the Kellogg Shale [*Kanaya*, 1957; *Barron et al.*, 1984]. In addition, *Tapia and Harwood* [2002] report on Late Cretaceous diatoms from the Canadian Arctic and there is a substantial literature on the Cretaceous and Paleogene diatoms of Russia and Siberia [e.g., *Gleser*, 1994, 1996; *Radionova et al.*, 1994, 2003; *Radionova and Khokhlova*, 2000; *Oreshkina et al.*, 2004; *Strelnikova*, 2006].

[4] Knowledge of central Arctic Eocene diatoms has significantly improved by the recent discovery of ~100 m of early middle Eocene, biosiliceous sediments from the Lomonosov Ridge (LR; Figure 1) during the 2004 Integrated Ocean Drilling Program (IODP) Expedition 302, "The Arctic Coring Expedition" (ACEX). These organic-rich, finely laminated sediments represent perhaps the most significant discovery of Paleogene diatoms in nearly two decades (Figure 2a). The assemblages are diverse, well-preserved (exceptionally so in some intervals), and characterized by shallow water (neritic to coastal) marine species, a number of which are unique to ACEX. The diatoms occur in conjunction with other marine to brackish siliceous microfossils such as ebridians, silicoflagellates and endoskeletal dinoflagellates, but also with diverse assemblages of freshwater chrysophyte cysts which dominate in some intervals (Figure 2b).

[5] This rich and unique sediment archive provides an exceptional opportunity to study Eocene environments of the central Arctic from a siliceous microfossil perspective. This is an important realization, particularly in the absent of calcareous microfossils [*Expedition 302 Scientists*, 2006]. The location also allows study of an unusual paleoenvironment receiving perpetual daylight during summer and dark-

[1]Norwegian Polar Institute, Polar Environmental Centre, Tromsø, Norway.
[2]Department of Geology, University of Tromsø, Tromsø, Norway.
[3]Institute for Chemistry and Biology of the Marine Environment (ICBM), Oldenburg University, Oldenburg, Germany.
[4]Department of Earth and Environmental Sciences, Yamagata University, Yamagata, Japan.
[5]Department of Earth and Planetary Sciences, Nagoya University, Nagoya, Japan.

0883-8305/08/2007PA001485$12.00

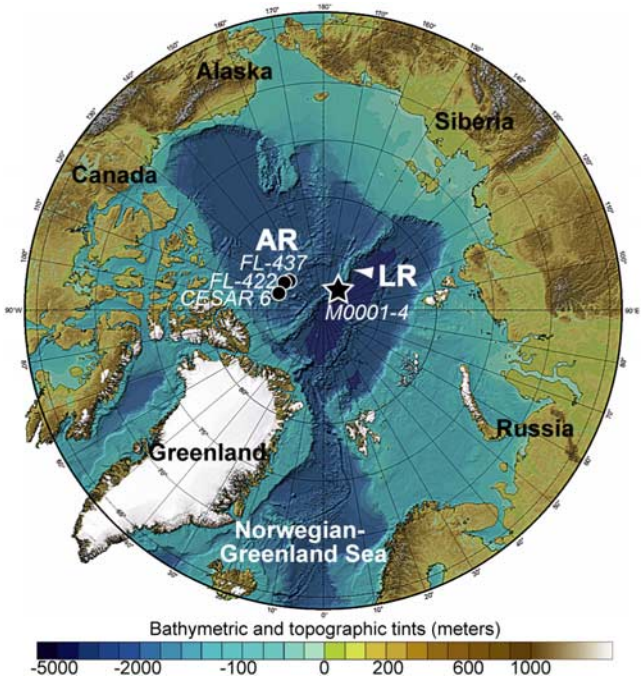

Figure 1. Integrated Ocean Drilling Program (IODP) 302 drill sites M0001-4 (star) at the Lomonosov Ridge (LR). Piston cores FL-422, FL-437 and CESAR 6 (circles) are indicated at the Alpha Ridge (AR). Base map: M. Jakobsson et al. (International Bathymetric Chart of the Arctic Ocean (IBCAO), Version 1.0, 2001, available at http://www.ngdc.noaa.gov/mgg/bathymetry/arctic/arctic.html).

ness during winter, as it does today. Palynology suggests the biosiliceous ACEX sediments are an expanded early middle Eocene section, i.e., ~50–45 Ma [*Backman et al.*, 2008]. This interval therefore represents an important phase in Cenozoic climate evolution—the start of the transition from greenhouse to icehouse conditions [*Zachos et al.*, 2001]. Knowledge of climatic and oceanographic variability in the Arctic region during this time is critical to achieving a broad understanding of the mechanisms of climate change through the transition. Although just a snapshot in time regarding siliceous microfossil history, much can be gleaned from this ~5 Ma window of preservation. In particular, the cooccurrence of marine and freshwater microfossils suggests an extraordinary depositional environment in which both marine and freshwater influences prevailed. In this paper, and with the backing of inorganic geochemistry, we explore these salinity changes from a siliceous microfossil (hereafter "silicofossil") perspective by quantifying changes in the dominance of silicofossil groups. These silicofossil associations, together with cooccurring and abundant brackish marine and freshwater tolerant dinoflagellate cysts (dinocysts) [*Expedition 302 Scientists*, 2006; *Brinkhuis et al.*, 2006; *Sangiorgi et al.*, 2008a], are key to understanding middle Eocene environments of the central Arctic. We also report on some intriguing compositional differences between some of the laminations comprising this extraordinary archive, which may give clues to the genesis of its formation. In the process we highlight the potential for paleoenvironmental reconstruction at different timescales.

2. Materials

[6] ACEX recovered sediment cores to 428 m below seafloor (mbsf) in water depths of ~1300 m, 250 km from the present-day North Pole [*Expedition 302 Scientists*, 2006]. Four closely spaced sites (M0001–M0004) (Figure 1) were drilled between 87°N and 88°N along the crest of the LR, a submarine block ~1500 km long and 150 km wide. Quaternary to Late Cretaceous (early Campanian) sediments were recovered (Figure 2) but which include a ~26 Ma hiatus from middle Eocene to early Miocene [*Sangiorgi et al.*, 2008b]. We use meters composite depth (mcd), with the exception of Figure 2 which is drawn by meters below seafloor (mbsf). Shipboard and onshore investigations indicate that silicofossils are mainly preserved between 202.66 mbsf and 313.61 mbsf (202.10–313.61 mcd; cores 2A 47X-2, 40 through 4A 15X-CC), but with a significant coring gap between 302.73 and 313.35 mbsf/mcd (a total of ~100 m of biosiliceous sediment excluding coring gaps above ~302 mbsf/mcd). Silicofossil traces occur below 313.61 mbsf/mcd down to 318.96 mbsf/mcd (18X-CC). Above 202.10 mcd (in cores 45X and 46X), silicofossils occur in exceptionally low abundance [*Sangiorgi et al.*, 2008b].

[7] The highest levels of biogenic silica (biosilica), and the best silicofossil preservation, occur between 220.24 and 313.61 mbsf (223.56–313.61 mcd) (Figures 2 and 3), corresponding to Lithostratigraphic Unit 2 [*Expedition 302 Scientists*, 2006]: a very dark gray, mud-bearing, finely laminated, organic-rich biosiliceous ooze. Gamma Ray Attenuation (GRA) bulk density strongly reflects biosilica preservation, with significantly reduced density values corresponding to high biosilica levels (Figures 2 and 3). The last occurrence (LO) of the free-floating freshwater fern *Azolla* spp., is an assumed synchronous event occurring as far south as the southern North Sea, and helps constrain an age model in Unit 2. This event is dated at 48.6 Ma and occurs at 299.95 mcd within core 4A-11X (e.g., Figures 2

Figure 2. (left) Arctic Coring Expedition (ACEX) core recovery, lithology, age model, and bulk density showing the window of biosilica preservation recorded in Holes 2A (87°55.271′N; 139°21.901′E; 1209 m water depth) and 4A (87°51.995′N; 136°10.641′E; 1288 m water depth). Core recovery, lithology, and Gamma Ray Attenuation (GRA) bulk density (g/cm^3) are redrawn from *Expedition 302 Scientists* [2006]. (right) Example SEM images of the silicofossil content. (a) Diatom-dominated interval (e.g., core 2A 57X), dominated by the diatom *Anaulus arcticus* (segmented structures in valve and girdle view, An) with some *Hemiaulus* spp. (He), *Porotheca danica* (Pd), *Stephanopyxis* spp. (St), and a few large chrysophyte cysts (white arrows); (b) Ebridian and chrysophyte cyst-dominated interval (e.g., core 4A 11X). Ebridians are the spongy structures, and chrysophyte cysts the rounded and flask-shaped spiny structures (white arrows). There are also a few silicoflagellates and diatoms in this image. Scale bar = 50 μm on both images.

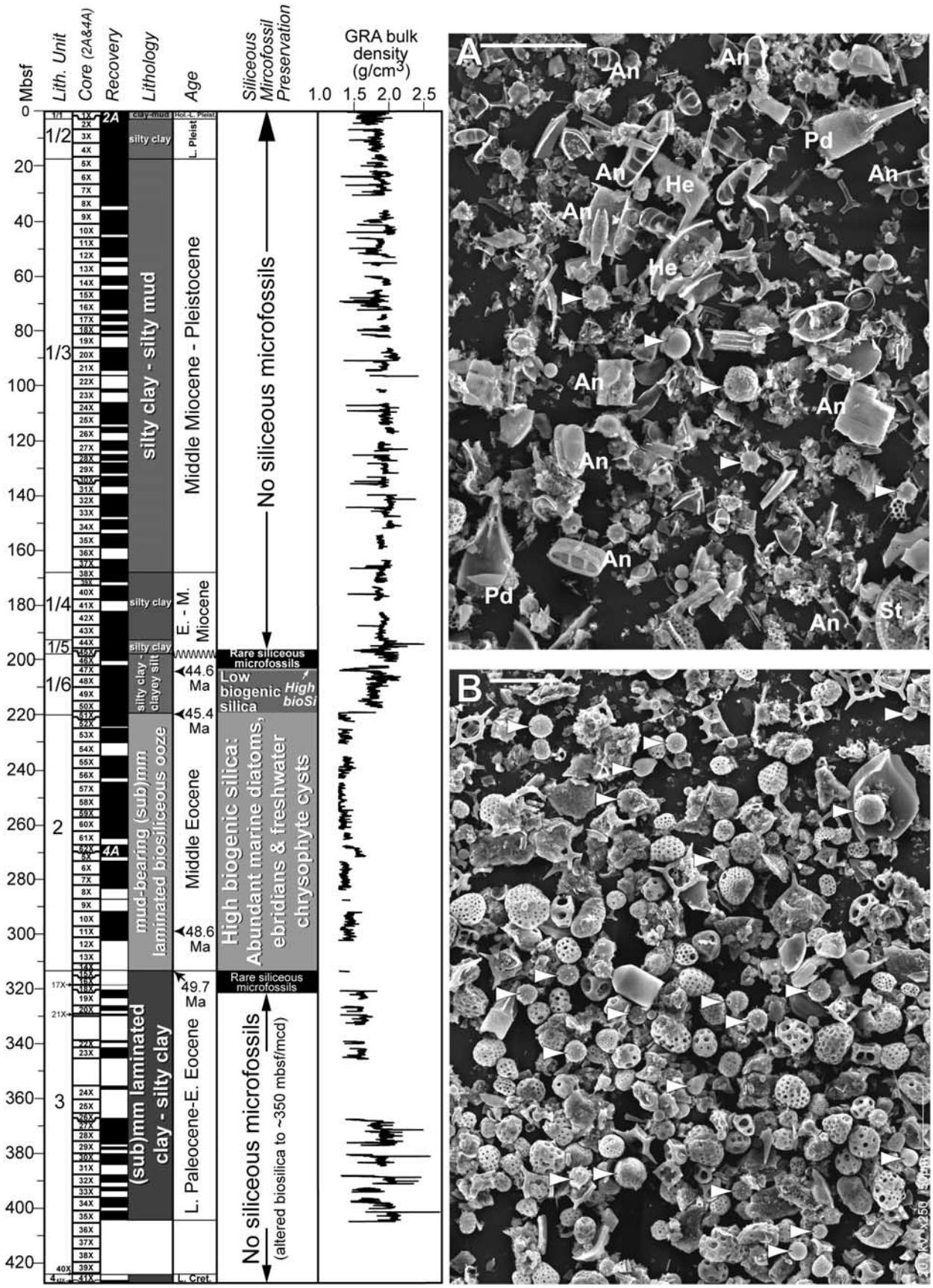
Mbsf
Lith. Unit
Core (2A&4A)
Recovery
Lithology
Age
Siliceous Mircofossil Preservation
GRA bulk density (g/cm3)
1.0 1.5 2.0 2.5
silty clay - silty mud
Middle Miocene - Pleistocene
L. Pleist.
silty clay
E. - M. Miocene
silty clay - clayey silt
mud-bearing (sub)mm laminated biosiliceous ooze
Middle Eocene
(sub)mm laminated clay - silty clay
L. Paleocene-E. Eocene
L. Cret.
No siliceous microfossils
Rare siliceous microfossils
Low biogenic silica
High bioSi
High biogenic silica: Abundant marine diatoms, ebridians & freshwater chrysophyte cysts
44.6 Ma
45.4 Ma
48.6 Ma
49.7 Ma
No siliceous microfossils (altered biosilica to ~350 mbsf/mcd)
A
B
An
Pd
He
St

Figure 2

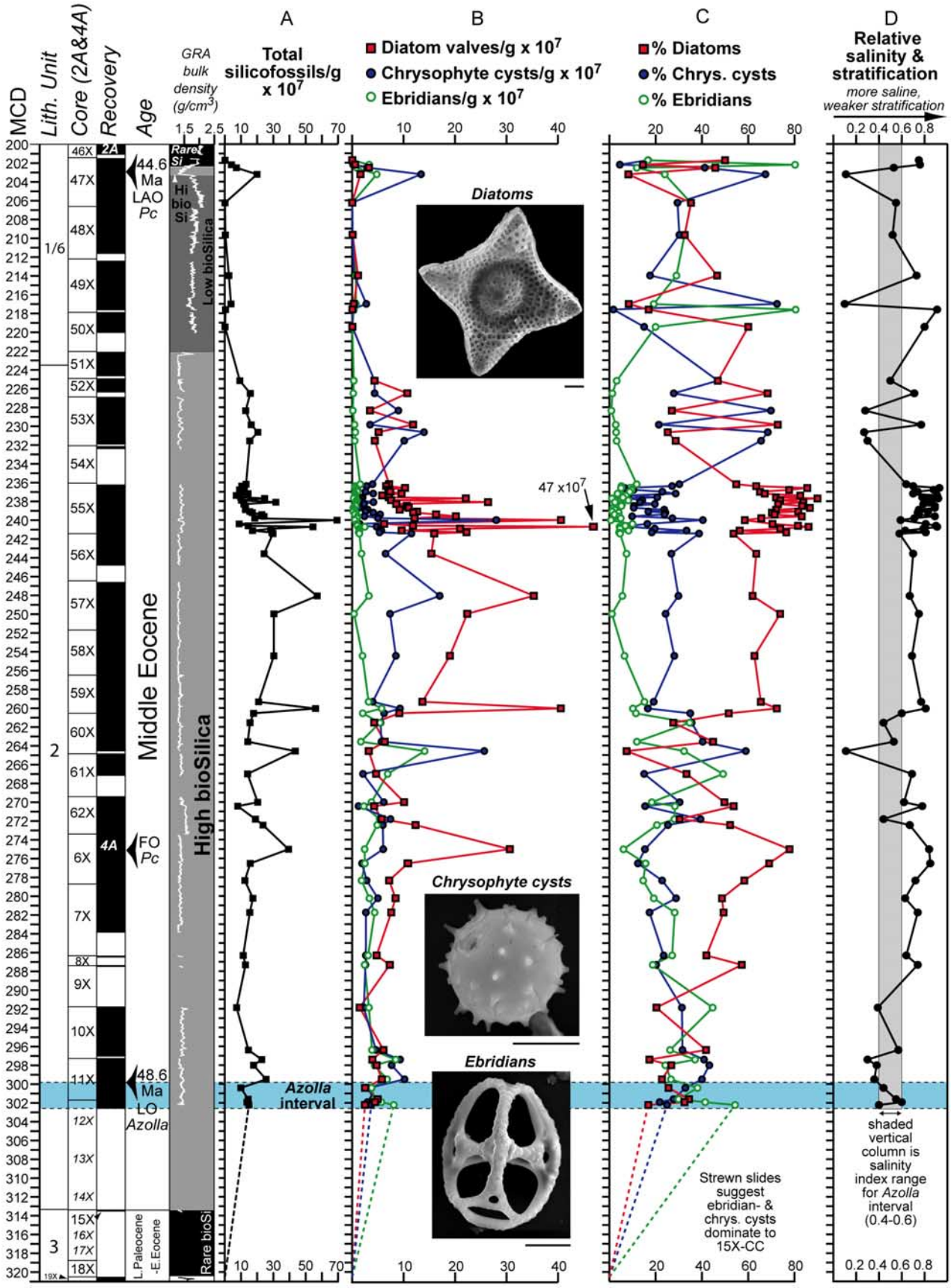
MCD
Lith. Unit
Core (2A&4A)
Recovery
Age
GRA bulk density (g/cm3)
A
Total silicofossils/g x 10^7
B
Diatom valves/g x 10^7
Chrysophyte cysts/g x 10^7
Ebridians/g x 10^7
C
% Diatoms
% Chrys. cysts
% Ebridians
D
Relative salinity & stratification
more saline, weaker stratification
Rare Si
Hi bio Si
Low bioSilica
High bioSilica
Rare bioSi
44.6 Ma LAO Pc
FO Pc
48.6 Ma LO Azolla
Middle Eocene
L.Paleocene -E.Eocene
Diatoms
Chrysophyte cysts
Ebridians
47 x10^7
Azolla interval
Strewn slides suggest ebridian- & chrys. cysts dominate to 15X-CC
shaded vertical column is salinity index range for Azolla interval (0.4-0.6)

Figure 3

and 3) [*Backman et al.*, 2008]. *Azolla* spp. are also found in the core catcher of core 4A-12X but not in core 4A-15X or below [*Brinkhuis et al.*, 2006], hence the "*Azolla* interval" (e.g., Figure 3) refers to the stratigraphic section which includes at least core 4A-12X upward to its LO, but which may extend downward to somewhere within the coring gap above 4A-15X. Rare occurrences of *Pyxilla oligocaenica* and *Brightwellia hyperborea*, age-diagnostic diatoms from the Norwegian-Greenland Sea and North Atlantic respectively [*Dzinoridze et al.*, 1978; *Gombos*, 1982, 1987; *Fenner*, 1985], confirm an early middle Eocene age as do sporadic, but very rare occurrences of *Macrora barbadiensis* [e.g., *Fenner*, 1985] throughout most of Unit 2. Other middle Eocene age-diagnostic diatoms are absent from the ACEX sediments.

[8] Above Unit 2, Lithostratigraphic Subunit 1/6, pyrite-rich, very dark gray silty clay (198.70–223.56 mcd), contains moderate to low levels of biosilica. However, the short interval at ~202.5–203.5 mcd represents a curious return to high levels of biosilica, reflected in a strong low-density spike (Figures 2–3). This high-biosilica interval occurs just ~40 cm below the very topmost level of biosilica preservation, providing a final, brief glimpse into silicofossil paleoenvironments before the record is lost altogether. Although there is no established central Arctic diatom biostratigraphy and correlations with regional sites are not obvious, diatoms may suggest a late middle to early late Eocene age in the ~202.5–203.5 mcd interval [*Backman et al.*, 2008]. However, the last abundant occurrence (LAO) of dinocyst *Phthanoperidinium clithridium* (Pc), occurring at 202.95 mcd, gives a consistently early middle Eocene age (44.6 Ma) (e.g., Figures 2 and 3). *Backman et al.* [2008] provide a brief discussion on this discrepancy. Using LO *Azolla* spp. and LAO *P. clithridium,* the sedimentation rate of the biosiliceous interval is ~2.43 cm/ka. By this age model the base of Unit 2 (313.61 mcd) is 49.7 Ma, and the base of Subunit 1/6 (223.56 mcd) is 45.4 Ma [*Backman et al.*, 2008] (Figure 2).

3. Methods

3.1. Silicofossil Analysis

[9] Seventy-six sediment samples were analyzed between 201.72 and 320.55 mcd (cores 2A 47X and 4A 11X) at an average 1.3 m resolution (lowest 11 cm; highest 5.73 m over a coring gap between cores 2A 50X and 52X). Sampling density within core 2A 55X is ~20 cm throughout, the detailed analysis of which are intended for a related contribution [*Sangiorgi et al.*, 2008a]. For silica-selective processing these organic-rich, carbonate-poor sediments required only oxidation of organic matter (hot 30% hydrogen peroxide) and removal of clays. For quantitative analysis, 1 ml of divinylbenzene microspheres (concentration 3.28×10^6 spheres/ml) was added to each of the digested samples prior to slide preparation [*Battarbee and Kneen*, 1982]. Since the current age model forces sedimentation rates to remain constant through the biosiliceous interval, we take our absolute abundance data (silicofossil/g) to be an indicator of flux (silicofossil/cm^2/ka). However, because of the outstanding age model issues, we favor discussion in terms of abundance, rather than flux. We consider the limitations in doing this but feel these do not affect our data interpretation greatly, particularly for Unit 2. Sediment recovery in cores 4A 12X, 15X and 18X was very poor (e.g., Figure 3) [*Expedition 302 Scientists*, 2006] and unavailable for processing. However, we supplement our study from strewn slides of cores 4A 15X-CC and 18X-CC taken from splits of shipboard digested sediments (provided by H. Brinkhuis/A. Sluijs, Utrecht University).

[10] Slides were analyzed for their silicofossil content at magnification ×1000 using a Zeiss Axioplan microscope with Plan-NEOFLUAR objectives. The following five groups were encountered and tallied: diatoms (both resting spores and vegetative valves), chrysophyte cysts, ebridians, silicoflagellates and siliceous endoskeletal dinoflagellates (e.g., actiniscidians). We counted at least 500 individual silicofossils per sample and additionally scanned for rare specimens at magnification ×100, ×400 and ×1000 to capture both very large and very small silicofossils.

3.2. Inorganic Geochemical Analysis

[11] We supplement our silicofossil data with geochemical proxies that may help indicate salinity or nutrient changes. Quantitative XRF analyses were performed on freeze-dried and homogenized (agate ball mill) sample powders. 600 mg of sample were mixed with 3600 mg of a mixture of dilithiumtetraborate/lithiummetaborate (50% $Li_2B_4O_7$/50% $LiBO_2$), preoxidized at 500°C with NH_4NO_3 (p.a.), and fused to glass beads. These were analyzed for major and minor elements using a Philips PW 2400 X-ray spectrometer. Analytical precision and accuracy were better than 5% for the elements Si, Ti, Al, Fe, and Mn, as checked by in-house and international reference rocks.

4. A Window of Biosilica Production and Preservation

[12] The biosiliceous ACEX sediments correspond to ~30% of the entire drilling recovery (Holes 2A + 4A), yet they represent the only window of preservation for biosilica in the last ~65 Ma in the central Arctic. Biosilica is present in Upper Cretaceous sediments in this region [e.g., *Bukry*, 1984, 1985; *Barron*, 1985; *Dell'Agnese and Clark*, 1994; *Davies*, 2006], yet it is not preserved again in the central Arctic until the early middle Eocene (this paper),

Figure 3. Silicofossil group abundance changes. (a) Absolute abundance of all silicofossils $\times 10^7$ per gram dry weight. Total includes diatoms, chrysophyte cysts, ebridians, silicoflagellates, and actiniscidians. (b) Absolute abundance changes in diatoms, chrysophyte cysts, and ebridians $\times 10^7$ per gram dry weight. Images: Diatom = *Trinacria* sp.; Chrysophyte cyst = a moderately ornamented "small" morphotype with visible pore; Ebridian = *Ammodochium fletcheri*. Scale bar = 10 μm. (c) Relative abundance changes in diatoms, chrysophyte cysts, and ebridians. Percentages are calculated from a total which includes these three groups plus silicoflagellates and actiniscidians. (d) Relative salinity and stratification index are based on the ratio diatoms/(chrysophyte cysts + diatoms).

and only then for ~5 Ma before its loss from the record. Why should biosilica be preserved in the central Arctic only during the early middle Eocene for the entire Cenozoic? Preservation of biosilica involves several factors: production and flux rates, depositional setting and biogeography, water mass exchanges as well as synsedimentary and diagenetic processes. The Arctic Paleocene and early Eocene no doubt supported biosilica production at some level, as suggested by rare pyritized specimens and altered biosilica below the preservation boundary (Figure 2) [*Expedition 302 Scientists*, 2006]. Its absence in the record (at least at the LR) during these times suggests one or a combination of the following: (1) reduced biosilica production, (2) reduced biosilica flux, perhaps a result of intense remineralization in Si-poor waters, and likely catalyzed by elevated temperatures; e.g., summer sea surface temperature (SST) estimates derived from the tetra-etherlipid index with 86 carbon atoms (TEX_{86}) index for the central Arctic are ~15°C for the Late Cretaceous [*Jenkyns et al.*, 2004] rising to ~18°C for the latest Paleocene and over 23°C for the Paleocene-Eocene thermal maximum (PETM) [*Sluijs et al.*, 2006], and (3) post sedimentary diagenetic alteration.

[13] Near the start of the middle Eocene, conditions changed that permitted accumulation and preservation of biosilica again; local and global changes triggered production and altered seawater and pore water chemistry. For example, while the causes are still debated, global changes to the Si cycle in the Eocene resulted in more silicic acid in the worlds oceans [e.g., *Yool and Tyrrell*, 2005], which not only gave diatoms, and other silica-secreting organisms, the Si required for growth but also slowed dissolution rates. The consequence was enhanced biosilica accumulation at the start of the middle Eocene, which lasted for ~4 Ma resulting in "Horizon A^C", a layer of biosilica-rich sediments known from the North Atlantic and equatorial Pacific [*McGowran*, 1989; *Yool and Tyrrell*, 2005]. It may be no coincidence that biosilica accumulation on the LR occurred at the same time as that for "Horizon A^C". Although the Arctic Ocean was relatively isolated at this time [*Moran et al.*, 2006], periodic flushing with Si-saturated waters from the North Atlantic may well have been possible allowing increased Si concentrations of deeper Arctic waters. Seasonal mixing events would have subsequently brought Si to the photic zone. With a system primed with Si, the final trigger may have been via locally elevated levels of Fe, a biolimiting nutrient well known to dramatically stimulate diatom blooms [e.g., *Coale et al.*, 1996]. An intensified hydrological cycle in the Eocene Arctic [*Jahren and Sternberg*, 2002] served to increase river outflow of humic matter into the Arctic Ocean and the availability of Fe. It is not inconceivable under this regime that some of the Si may well have been locally sourced also.

[14] Factors permitting biosilica preservation would have also been important; temperature in particular. The age of the base of the biosiliceous sediments on the LR (i.e., base of Unit 2; ~50 Ma) corresponds to the very start of global cooling to icehouse conditions, following the end of the Early Eocene Climate Optimum (EECO) [*Zachos et al.*, 2001]. This correlation suggests falling temperatures may have dipped below a threshold level favorable for biosilica preservation. Locally reduced SSTs at this time are suggested by unpublished TEX_{86} SST estimates of ~12°C (A. Sluijs, personal communication, 2007) and ~10°C during the *Azolla* phase [*Brinkhuis et al.*, 2006] compared with a background Paleocene temperature of at least 17–18°C [*Sluijs et al.*, 2006].

[15] At ~45 Ma, biosilica is no longer preserved on the LR. This is tentatively linked with a shoaling of the ridge crest in response to either tectonic processes or regional sea level variations [*O'Regan et al.*, 2008] that ultimately led to the hiatus in the ACEX record (Figure 2) [*Sangiorgi et al.*, 2008b]. Not long after the ridge had subsided and the Fram Strait opened wide enough for deep water connection to the Atlantic [*Jakobsson et al.*, 2007], permanent sea ice had covered the region [*Moran et al.*, 2006; *St. John*, 2008].

5. ACEX Silicofossils

[16] The interplay of climatic, biogeographic and tectonic factors created conditions favorable for the production and preservation of biosilica on the LR during the early middle Eocene. This ~5 Ma window therefore reflects a truly unique phase in the Cenozoic depositional history of the ridge. The nature of the silicofossil content provides further insight into central Arctic paleoenvironments during this time. Diatoms, chrysophyte cysts and ebridians are by far the most abundant groups preserved in these sediments (54.5%, 28.3% and 14.6%, respectively), while silicoflagellates and actiniscidians occur in comparatively minor abundance (1.8% and 0.8%, respectively). We consider the main groups next.

5.1. Diatoms

[17] Diatoms are unicellular, eukaryotic, photosynthetic golden brown algae with a preservable opaline frustule of two valves and a geological history extending back to at least the Early Cretaceous [e.g., *Harwood and Nikolaev*, 1995]. As one of the first groups to respond to an influx of nutrients (a "boom and bust" lifestyle), they are excellent eutrophic indicators and widely used as tools for paleoenvironmental reconstruction. The ACEX diatoms are well-preserved, shallow marine (e.g., "biddulphoid" types of *Hendey and Sims* [1984]), neritic taxa, most of which are heavily silicified resting spores or resting cells. Important taxa include *Anaulus arcticus*, *Costopyxis trochlea*, *Goniothecium danicum*, *Hemiaulus* spp. (both robust types with a highly domed central area, and less robust "typical" types), *Leptoscaphos levigatus* and *L. punctatus*, *Odontotropis* spp., *Porotheca danica*, *Pseudopyxilla* spp., *Pseudostictodicsus* spp., *Pterotheca aculeifera* and other species of this genus, *Pyxilla* spp., *Stellarima microtrias*, *Stephanogonia* spp., *Stephanopyxis* spp., *Trinacria* spp. and *Trochosira* spp. See *Suto et al.* [2008a, 2008b, 2008c] for taxonomic treatment of some of these taxa, a few of which are new species and combinations. Detailed diatom assemblage changes throughout the entire biosiliceous interval will be discussed elsewhere.

5.2. Chrysophytes and Chrysophyte Cysts

[18] Relatively little is understood about the ecology and lifecycle of chrysophytes but they are known to be photosynthetic algae (or mixotrophs) of mainly freshwater origin

associated with low to moderate productivity lakes and ponds. They also live in bogs, sea ice, [*Lipps and McCartney*, 1993], lake ice [e.g., *Smol*, 1988], and wet meadows [*Adam and Mahood*, 1981]. They can dominate in dilute brown (acidic) waters where they prosper because of their ability to out-compete other algae for P when it is limiting [*Nicholls and Wujek*, 2003]. Although the group (and their cysts) may give an indication of trophic status, the role of nutrients in stimulating chrysophyte blooms is not as well understood as it is for the diatoms. Temperature and pH effects, however, seem to be important for modern lake settings [e.g., *Zeeb and Smol*, 2001; *Nicholls and Wujek*, 2003]; an abundance of cysts generally indicating reduced temperatures.

[19] Chrysophyte cysts (or stomatocysts) are the preservable, endogenously formed resting stage, made of opaline silica. They are typically hollow with a single pore (a simple or collared hole) and are normally spherical, but also ovoid or even flask-shaped and may be smooth-walled or ornamented. They are usually 5–10 μm in diameter [*Lipps and McCartney*, 1993], but may be as small as 2.5 μm or as large as 30 μm [*Adam and Mahood*, 1981], making them on average smaller than the diatoms. Cyst formation is an obligatory part of the life cycle for all chrysophytes [e.g., *Hibberd*, 1977; *Skogstad and Reymond*, 1989]. After encystment, cysts sink through the water column and may germinate in response to favorable conditions [*Zeeb and Smol*, 2001]. Chrysophyte cysts, or at least their occurrences in marine sediments, have a fossil record extending back to at least the Early Cretaceous [*Harwood and Gersonde*, 1990] and they are known to be valuable paleoenvironmental indicators in fossil freshwater deposits [*Adam and Mahood*, 1981]. Although exclusively marine and brackish taxa do exist in modern environments (the artificially used Family Archaeomonadaceae based purely on their marine occurrence), they are considered rare [*Zeeb and Smol*, 2001, and references therein]. We judge the ACEX chrysophyte cysts to be of mostly freshwater origin, or at most, tolerant of weakly brackish salinities. We base our reasoning on the following: (1) The ACEX chrysophyte cysts are more akin in morphology, size, and diversity to modern freshwater chrysophyte cysts from lakes and *Sphagnum* bogs [e.g., *Adam and Mahood*, 1981; *Duff et al.*, 1994; *Wilkinson et al.*, 2002] than they are to fossil (presumed) marine types recovered in marine Paleogene sediments, e.g., the southwest Pacific [*Perch-Nielsen*, 1975; *Hajós*, 1976] and South Atlantic [*Gombos*, 1977] and (2) they are very abundant in the ACEX sediments, which would be unusual for any normal marine setting. While these points alone do not preclude marine cysts, and we note it is pure speculation to base paleoecology on morphological similarities with modern counterparts, all considerations (discussed below) suggest low surface salinities existed throughout the period of biosilica accumulation on the LR, and therefore that the ACEX chrysophyte cysts are "likely" to have been of freshwater origin.

[20] We estimate at least 30 different morphotypes exist in the ACEX sediments and as far as we are aware, they represent the most diverse, abundant and sustained levels of fossil chrysophyte cysts ever discovered in a Paleogene setting. *Dell'Agnese and Clark* [1994] report up to 65% chrysophyte cysts (their "Archaeomonads") in the short middle Eocene piston core FL-422 on the Alpha Ridge but indicated a low diversity of just three types. During analysis of the ACEX cores we arbitrarily classified them according to their ornamentation, shape and size. Most of these morphotypes are extraordinarily well preserved retaining delicate spines and other ornamental features. It is not the subject of this paper to describe each morphotype but their size appears to be environmentally, perhaps stratigraphically important. We classify our "large" morphotypes as 10 μm or larger and "small" morphotypes as <10 μm. Generally, the large morphotypes have longer spines than the small types. Chrysophyte scales such as those found in Canadian submodern lake sediments [e.g., *Wolfe and Perren*, 2001] and those of middle Eocene age [*Siver and Wolfe*, 2005a, 2005b] are not encountered in the studied interval.

5.3. Ebridians

[21] Ebridians are silica-secreting zooflagellates, and the third silicofossil group we consider here. They are diverse in the ACEX sediments and *Onodera et al.* [2008] report on their paleoecology and paleoceanography. Ecological information on ebridians is scarce because of the rarity of extant species, however all living and fossil ebridians are considered to be marine, inhabiting neritic to coastal environments. They are important in low-salinity brackish waters such as estuaries, embayments, close to river mouths [e.g., *Ernisse and McCartney*, 1993] and inland seas (e.g., the Black Sea) [*Osawa et al.*, 2005], although they are also reported from normal marine salinity (paleo)settings of the Paleogene (e.g., Kerguelen Plateau) [*Bohaty and Harwood*, 2000]. Living ebridians are opportunistic, herbivorous grazers feeding on diatoms and dinoflagellates [*Hargraves*, 2002; *Hoppenrath and Leander*, 2006], and may undergo sporadic population explosions under favorable conditions in summer, e.g., Long Island Sound and the Nile River [e.g., *Ernisse and McCartney*, 1993]. Their fossil record is patchy but they first appear in the Cretaceous [e.g., *Hoppenrath and Leander*, 2006] are most common in Paleogene sediments [e.g., *Bohaty and Harwood*, 2000, and references therein], declining after the late Miocene [e.g., *Ernisse and McCartney*, 1993].

5.4. Silicofossil Group Abundance Changes in the ACEX Sediments

[22] Figure 3 illustrates abundance changes for total silicofossils and the three main groups. Silicofossils are abundant on the order of $\times 10^7$–10^8 specimens/g (Figure 3a). This is a factor higher than that reported by *Brinkhuis et al.* [2006] for the *Azolla* interval (shaded horizontal bar, Figure 3). We illustrate abundance data for the three main groups in Figures 3b–3c. Total silicofossil abundance reflects Si/Al reasonably well (Figure 4) ($R^2 = 0.3$; Figure 5a) where Unit 2 is characterized by very high values and Subunit 1/6 by very low values. The ~202.5–203.5 mcd interval is conspicuous by a Si/Al peak (Figure 4). Silicofossil abundance (Figure 3a) steadily increases from the base of Unit 2 to maximum levels (~69×10^7 specimens/g) at ~240 mcd within core 2A 55X. Above ~240 mcd abundance falls off to minimum levels throughout most of

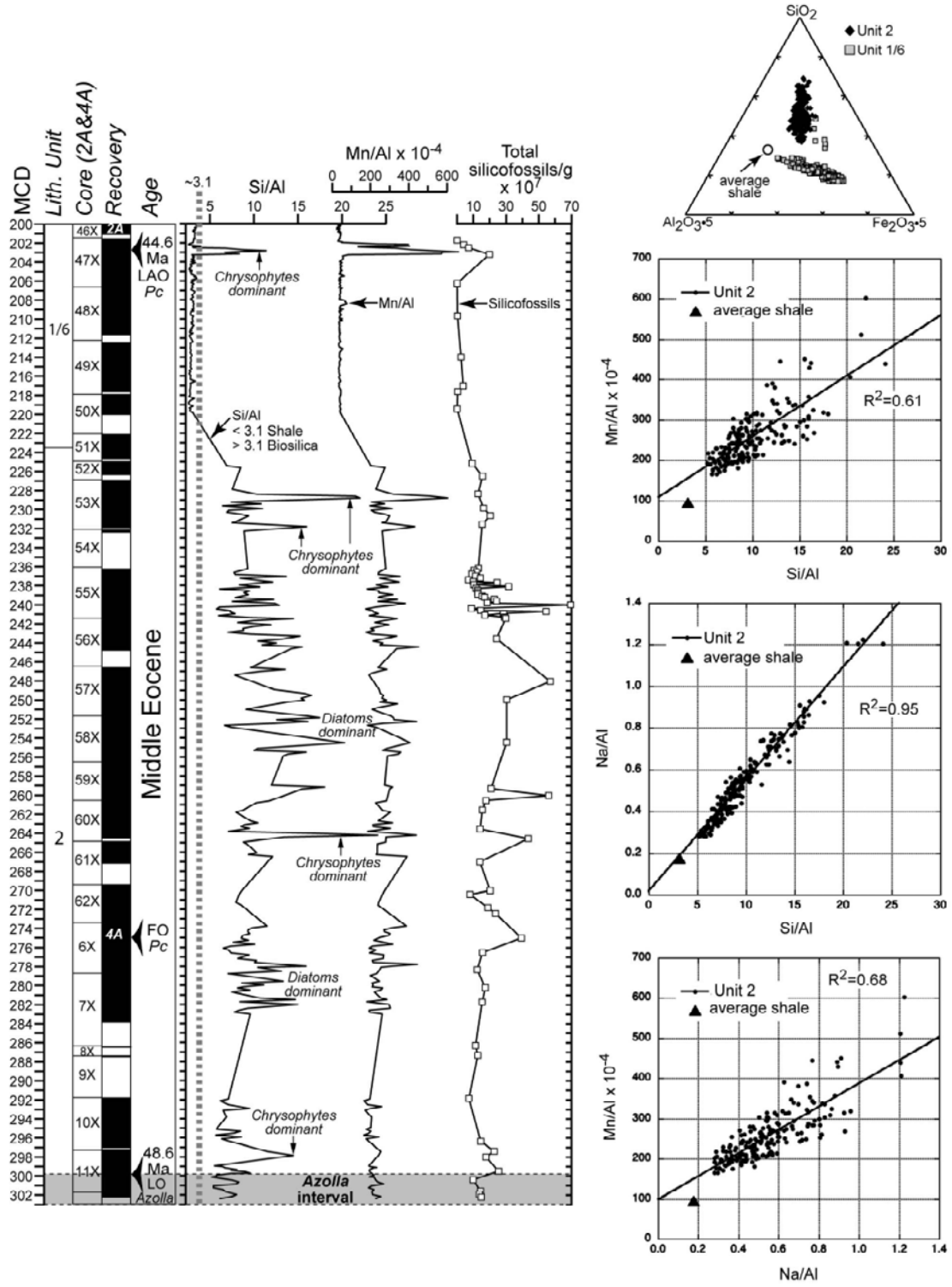

Figure 4. Relationships between the elemental ratios Si/Al, Mn/Al, and silicofossil abundance. Triangle diagram shows compositional differences between Unit 2, a mixture of average shale (circle) and SiO_2, and Subunit 1/6, a mixture of average shale with a significantly Fe-enriched (pyrite) phase. Si/Al is 3.1 for average shale [*Wedepohl*, 1971]; hence Si/Al enrichments over this value indicate the presence of biosilica (unaltered and altered) and quartz (unlikely in the studied interval). Curiously, chrysophyte cysts represent the highest Si/Al anomalies. Scatterplots at right indicate relationships between elemental ratios.

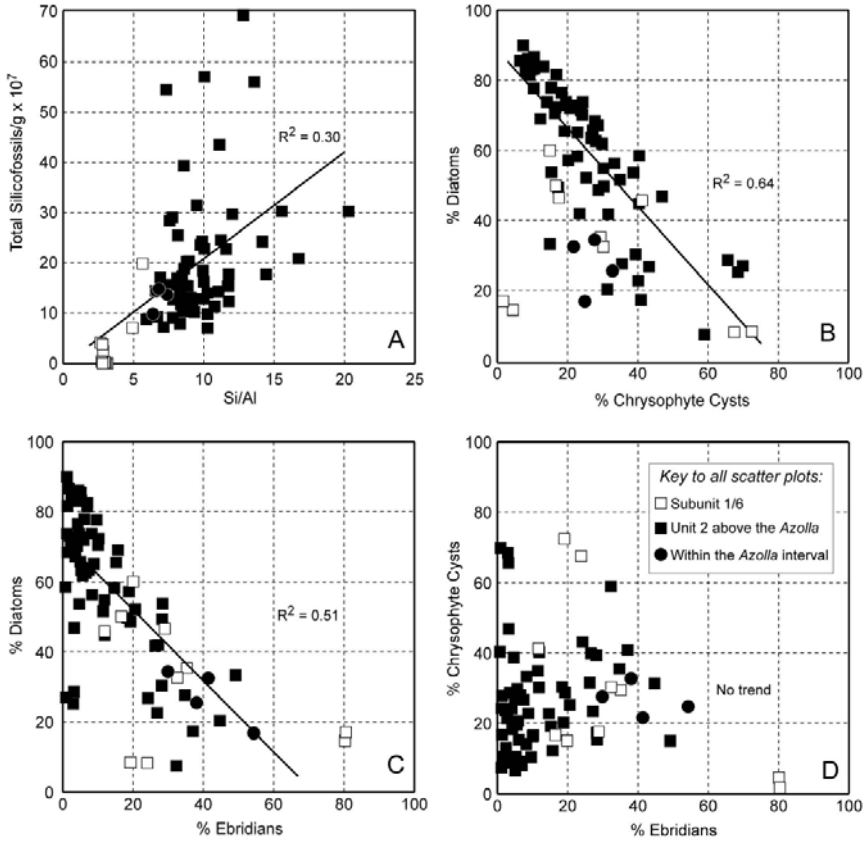

Figure 5. Scatterplots indicating relationships between (a) total silicofossil abundance and the elemental ratio Si/Al (averaged across sampling intervals) and (b–d) silicofossil group abundance.

Subunit 1/6 (average $\sim 4 \times 10^7$ specimens/g). This overall trend is punctuated by some noteworthy biosilica maxima, particularly just after the *Azolla* interval, at ~275 mcd, ~265 mcd, ~260 mcd and ~248 mcd. Because of coring gaps sampling resolution is relatively low in some intervals and there may be other biosilica maxima in the record not identified in this study. The maxima just after the *Azolla* interval and at ~265 mcd comprise mainly chrysophyte cysts and ebridians (Figures 2b, 3b, and 3c), while the maxima at ~275 mcd, ~260 mcd and ~248 mcd are caused by an overall dominance in diatoms (Figures 2a, 3b, and 3c). The maximum peak at ~240 mcd also comprises mostly diatoms but chrysophyte cysts are also important here. In Subunit 1/6, the ~202.5–203.5 mcd interval comprises mainly chrysophyte cysts (Figures 3b, 3c, and 4). We also note some interesting meter- to centimeter-scale cyclicities in group dominance, e.g., relative abundance (%) changes (Figure 3c) in cores 2A 49X, 52–53X and 60–62X.

[23] Our diatom abundance estimates on the order of $\times 10^7$–10^8 valves/g are comparable to lower estimates in modern upwelling systems and Quaternary high-flux regions (e.g., coastal Antarctica, Gulf of California). Similar estimates of up to 40×10^7 specimens/g were given for the Alpha Ridge middle Eocene core FL-422 by *Dell'Agnese and Clark* [1994]. A noteworthy point is that in those intervals where diatoms dominate, they nearly always do so at greater absolute abundance (up to $\sim 47 \times 10^7$ valves/g) than that for corresponding intervals of chrysophyte cyst dominance (up to $\sim 28 \times 10^7$ cysts/g) or ebridian dominance (up to $\sim 14 \times 10^7$ specimens/g) (Figure 3b). Also, diatom dominance is sustained over much longer intervals than it is for chrysophyte cysts or ebridians. We find no preservational bias between groups by our methods, hence this is likely a reflection of the diatoms being more efficient producers (bloomers) than the other groups if production of all silicofossil groups is considered in situ.

[24] Our chrysophyte cyst abundance estimates on the order of $\times 10^7$ cysts/g are relatively high. For example, typical cyst abundance for subfossil lake sediments may be a factor lower, i.e., $\times 10^6$ cysts/g [e.g., *Edlund and Stoermer*, 2000] (Quaternary Lake Baikal sediments). It is difficult to find absolute abundance data for Paleogene cysts or older, but *Cornell* [1972] estimates cyst abundance on the order of $\times 10^6$ cysts/g from the Upper Cretaceous Marca Shale, California. Considered by cells/g, chrysophytes may well outnumber diatoms in the ACEX sediments but since it is highly unlikely that the diatom valves counted represent 50:50 epivalve:hypovalve (even if they belonged to the same diatom cell) this cannot be assumed.

6. Environmental Setting in the Early Middle Eocene Arctic

[25] Unit 2 and Subunit 1/6 are partly defined on high total organic carbon (TOC) values of >2.2 wt% compared with moderate to low TOC values in overlying sediments

and variable TOC below Unit 2 [*Expedition 302 Scientists*, 2006; *Brumsack et al.*, 2007]. In modern environments, TOC-rich sediments accumulate in euxinic basins (e.g., the Black Sea) and coastal upwelling regions (e.g., Gulf of California). Similarly, Black Sea-type deposition under estuarine circulation is suggested for the Paleogene ACEX sediments including the biosiliceous interval [*Stein et al.*, 2006; *Brumsack et al.*, 2007]. *Stein et al.* [2006] show how these organic-rich, finely laminated sediments were deposited under euxinic-anoxic conditions caused by a positive freshwater balance and salinity stratification. Here, we demonstrate that they also contain high abundances of marine to brackish and freshwater silicofossils. Having outlined broad-scale changes in dominance of the three main groups, we suggest that diatoms, chrysophyte cysts and ebridians can provide valuable information on changes in salinity, water stratification and trophic status.

6.1. Salinity and Stratification

[26] Salinity fluctuations on silicofossil evidence affected the central Arctic in the Late Cretaceous [see *Davies*, 2006, for review]. In the Eocene Arctic, elevated humidity [*Jahren and Sternberg*, 2003] and precipitation [e.g., *Jahren and Sternberg*, 2002] lead to enhanced river runoff and fresher surface waters than today. Freshwater discharges have already been suggested for creating stratification and anoxia at depth during biosiliceous deposition [*Stein et al.*, 2006]. However, our silicofossil data provide necessary paleoecological perspective on this reconstruction.

[27] Diatom abundance is generally negatively correlated to both chrysophyte cysts (R^2 = 0.64; Figure 5b) and ebridians (R^2 = 0.51; Figure 5c). Chrysophyte cyst and ebridian abundance, however, do not appear to be correlated (no trend; Figure 5d). By this reasoning, we suggest the ratio diatoms/(chrysophyte cysts + diatoms) can be used to assess relative salinity and degree of stratification. This relative salinity index is indicated by depth in Figure 3d and by age in Figure 6. Given that the Arctic Ocean was still relatively isolated during this time, we argue for variation between "fresher, stronger stratification (deeper halocline or more stable)" and "more saline, weaker stratification (shallower halocline or more mixed)" within an overall brackish environment, rather than variation between fully freshwater (i.e., salinities not below <0.5‰) or fully marine (i.e., salinities not above 35‰).

[28] Our suggested paleosalinity reconstruction corresponds reasonably well to both quantitative salinity changes (from δ^{18}O-derived fish bone carbonate) provided by *Waddell and Moore* [2008] and to crude shipboard-based palynology count data [*Expedition 302 Scientists*, 2006] analyzed here (Figure 6). Clearly our salinity index could be improved by considering species changes rather than by group. One consideration might be for the diatom *Anaulus arcticus* newly described by *Suto et al.* [2008c]. Although thought of as marine it may well have had a lower-salinity tolerance than the other ACEX diatoms if it occupied the same environmental niche as modern species of this genus known to be littoral or "surf zone" bloomers [*Talbot and Bate*, 1986; *Hewson et al.*, 2001], i.e., if it lived coastally and proximal to a river mouth, for example. Regardless, fully freshwater middle Eocene diatoms such as that described from the Canadian Northwest Territories by *Wolfe and Edlund* [2005] and *Siver and Wolfe* [2007] are apparently not present in the ACEX sediments. This gives some confidence to our methodology.

[29] The shaded vertical columns in Figures 3d and 6 indicate the salinity (index) range for the *Azolla* interval, providing a means to gauge the significance of values outside of this range. During the *Azolla* phase, freshening episodes lowered surface salinities to below at least (presumably) ~1–1.6‰ but no greater than 5‰, on the basis of salinity tolerances of living *Azolla* [*Brinkhuis et al.*, 2006, and references therein]. The higher-salinity estimates derived from fish bones for the *Azolla* interval (Figure 6) are due to alteration at the sediment water interface [see *Waddell and Moore*, 2008]. Nonetheless, the trends, rather than the values are focal here and our qualitative data confirm lower salinity (stronger stratification) during the *Azolla* phase, and a brief incursion of more saline water ~100–150 ka after the demise of *Azolla* (i.e., ~48.5 Ma) rather than directly at its termination (i.e., ~48.6 Ma) as postulated by *Brinkhuis et al.* [2006]. This incursion is indicated by a relative increase in diatoms diagnostic of shallow water exchange with the North Atlantic since the connection between the Arctic Ocean and the Western Siberian Sea (Turgay Strait) had presumably closed slightly earlier (earliest middle Eocene) [*Radionova and Khokhlova*, 2000].

[30] Our data suggest further fluctuations in salinity throughout Unit 2, with two notable phases of higher salinity (1) from ~48.1 to ~47.5 Ma (~287–272 mcd) and (2) from ~47 to just later than ~46 Ma (~260–236 mcd) (Figures 3d and 6). Both phases of increased salinity are also apparent in the palynology data and partly the fish bone data albeit at lower resolution than our silicofossil data. The latter phase includes the initiation of sea ice (at 46.25 Ma) [*St. John*, 2008] corresponding closely to the first abundant appearance (FAO) of curious, finely silicified, needle-like

Figure 6. Salinity changes during middle Eocene biosilica accumulation on the LR. Our salinity data (left) are compared with those derived from palynomorph abundance data (center) and from fish bone carbonate (right). Relative abundance of freshwater (FW) algae and FW tolerant dinocysts is calculated from raw count data published by *Expedition 302 Scientists* [2006] from a total of nonterrestrial palynomorphs. All positively identified nonterrestrial palynomorphs are considered FW tolerant except the following dinocyst genera which are considered marine (H. Brinkhuis, personal communication, 2007): *Operculodinium, Spiniferites* and *Thalassiphora*. Palynomorph data are based on counts of core catcher material processed on-ship and hence indicate broad changes only. Far left column indicates changes in dominance of the three main silicofossil groups: C = chrysophyte cysts; D = diatoms; E = ebridians. *Eldrett et al.* [2004] date the First Occurrence (FO) *P. clithridium* at 46.1 Ma for the Norwegian-Greenland Sea, yet the age model of *Backman et al.* [2008] suggests an earlier age (47.5–47.7 Ma) for the Arctic.

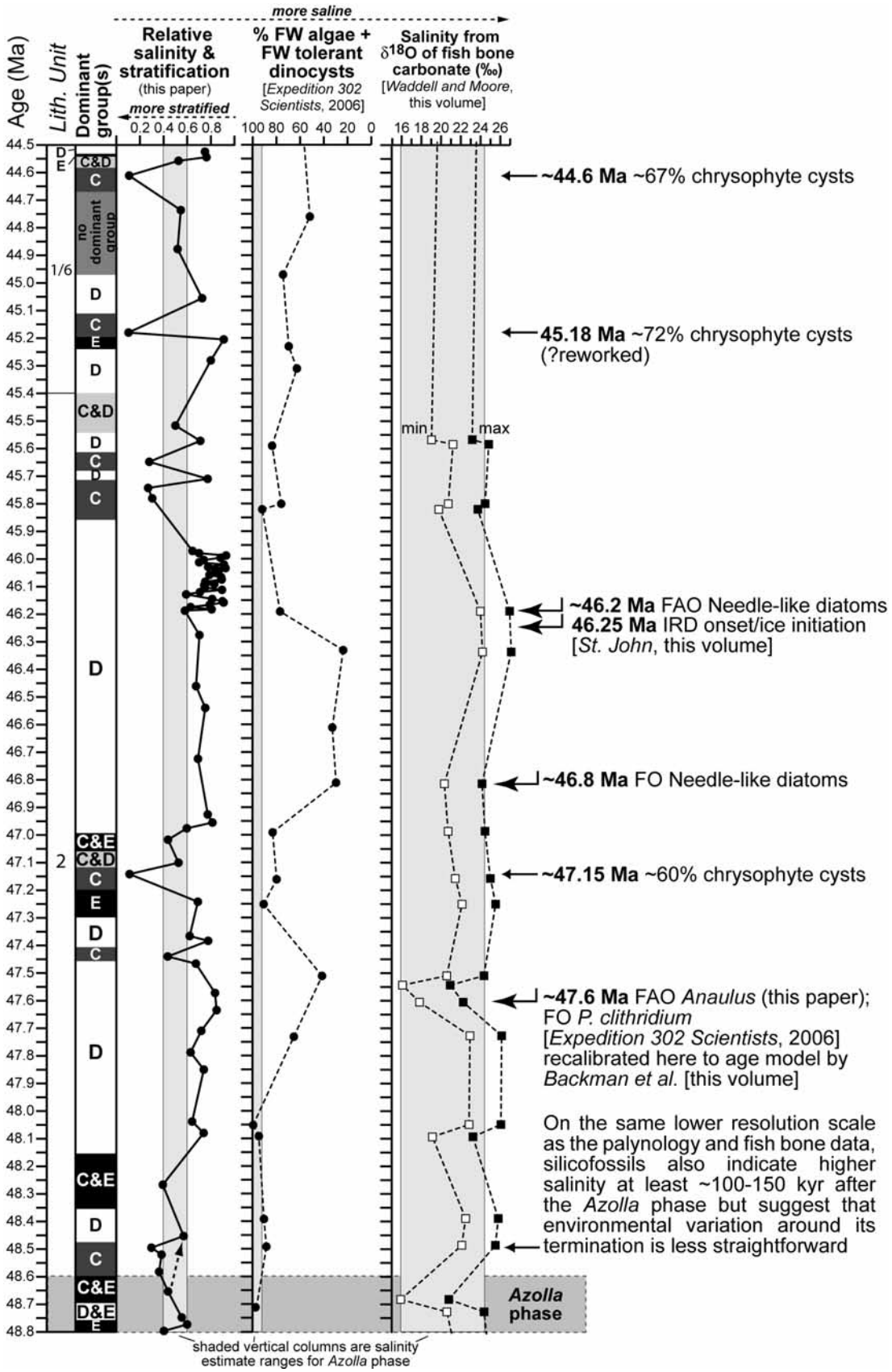
more saline
Age (Ma)
Lith. Unit
Dominant group(s)
Relative salinity & stratification (this paper)
more stratified
0.2 0.4 0.6 0.8
% FW algae + FW tolerant dinocysts [Expedition 302 Scientists, 2006]
100 80 60 40 20 0
Salinity from δ18O of fish bone carbonate (‰) [Waddell and Moore, this volume]
16 18 20 22 24 26
~44.6 Ma ~67% chrysophyte cysts
45.18 Ma ~72% chrysophyte cysts (?reworked)
min
max
~46.2 Ma FAO Needle-like diatoms
46.25 Ma IRD onset/ice initiation [St. John, this volume]
~46.8 Ma FO Needle-like diatoms
~47.15 Ma ~60% chrysophyte cysts
~47.6 Ma FAO Anaulus (this paper); FO P. clithridium [Expedition 302 Scientists, 2006] recalibrated here to age model by Backman et al. [this volume]
On the same lower resolution scale as the palynology and fish bone data, silicofossils also indicate higher salinity at least ~100-150 kyr after the Azolla phase but suggest that environmental variation around its termination is less straightforward
Azolla phase
no dominant group
shaded vertical columns are salinity estimate ranges for Azolla phase

Figure 6

diatoms occurring in exceptionally high abundance (up to ~33.3 valves/g × 10^7; ~71 % of total diatoms). They are the subject of another contribution but may be one of the more important vegetative diatoms in the ACEX sediments indicating an extraordinary depositional environment that allowed exceptional preservation. The intervening period ~47.5 to ~47 Ma appears to be a phase of surface freshening, or episodic freshening, on silicofossil evidence, which is also suggested by the palynology data, but only weakly by the fish bone data. A low-salinity spike at ~47.6 Ma identified in the fish bone data [*Waddell and Moore*, 2008] marks the First Occurrence (FO) of freshwater tolerant dinocyst *Phthanoperidinium clithridium* but the spike is not apparent either in the silicofossil data or in the overall palynology data. This may be partly down to sample resolution differences. However, ~47.6 Ma (~275 mcd) also marks the FAO of the diatom *Anaulus arcticus* where it comprises ~40% of the diatom assemblage. If *Anaulus arcticus* inhabited the surf zone in the Eocene as species of this genus do today, then it may be possible to assess sea level changes by its relative abundance. Indeed, *Waddell and Moore* [2008] suggest the low-salinity spike at ~47.6 Ma may correspond to the significant drop in sea level of perhaps 20–30 m estimated to have commenced at ~48 Ma by *Miller et al.* [2005]. Although these data suggest a correlation, clearly, higher-resolution data or perhaps refinement of the age model in Unit 2 is required to tie in the ACEX data with global sea level changes.

[31] Interpretation of Subunit 1/6 (later than ~45.4 Ma) is complicated but appears to be characterized by generally low salinity, particularly in the ~202.5–203.5 mcd interval (~44.6 Ma) prior to the eventual unroofing of the ridge described by detailed palynological data [*Sangiorgi et al.*, 2008b]. *Onodera et al.* [2008] suggest a shallow connection to the Atlantic on ebridian and silicoflagellate evidence for Subunit 1/6. We cannot confirm or deny this with our diatom data as, although the diatom assemblages in Subunit 1/6 are somewhat different from those in Unit 2 (C. E. Stickley, unpublished data, 2007), diatom abundance is very low (Figure 3b) and the derived salinity signal is noisy (Figure 6).

[32] With the possible exception of sea level–driven salinity changes at 49 Ma and 48 Ma [see *Waddell and Moore*, 2008, for discussion], fluctuations in salinity during biosilica deposition on the LR are most likely controlled by intensity of precipitation and river runoff. In addition, Mn/Al ratios are high in the biosiliceous interval (Figure 4) and may indicate an environment akin to the modern Baltic Sea where permanent stratification is caused by low-salinity (6–9‰) surface waters. High concentrations of dissolved Mn occur at the boundary between the oxic (upper) and anoxic (lower) water layers owing to intense Mn recycling and the presence of high dissolved Mn^{2+} concentrations in the anoxic water column. Episodic, oxygenated, salt water inflow from the North Sea causes abrupt changes from anoxic to oxic conditions in bottom waters at several years intervals [*Huckriede and Meischner*, 1996, and references therein], allowing Mn oxidization and deposition of Mn-rich minerals (fixation of Mn^{2+}-carbonates) in the sediments. A similar high-Mn scenario might be invoked for Unit 2 above the *Azolla* interval, where very high Mn/Al values indicate flushing periods and possibly increased salinity. The very low Mn/Al values in Subunit 1/6 indicate the opposite and a return to extensive anoxia with the exception of the 202.5–203.5 mcd interval. This assumption is corroborated by very high Fe/Al ratios which indicate anoxic water column conditions [*Lyons and Severmann*, 2006; *Brumsack*, 2006].

[33] Generally Mn/Al correlates reasonably well to silicofossil abundance and Si/Al (R^2 = 0.61) (Figure 4). Anoxic basins act as nutrient and Mn traps [*Konovalov and Murray*, 2001; *Brumsack*, 2006]. When anoxic conditions cease during flushing events, dissolved silica is made available for plankton growth, whereas Mn will be oxidized and converted into the particulate Mn^{4+} state. In the paleorecord both Mn and Si will accumulate in parallel. This seems to be the case in Unit 2 and the 202.5–203.5 mcd interval of Subunit 1/6. If analogous to the Baltic Sea, this may indicate some relative ventilation and additional nutrient supply during the main phase of biosilica production on the LR. Porosity (indicated by Na) is also an important factor for enrichment and may explain Mn/Al peaks (R^2 = 0.95 and 0.68 for Na/Al versus Si/Al and Mn/Al, respectively, Figure 4). We also note submillimeter laminations and a high abundance of palynomorphs throughout the biosiliceous interval [e.g., *Expedition 302 Scientists*, 2006], which shows that if ventilation occurred, it was not intense or only short-lived (e.g., subannual) in this landlocked sea. Ventilation intense enough to oxidize organic microfossils did not affect the region until the early Miocene [*Jakobsson et al.*, 2007].

6.2. Trophic Status

[34] Do the silicofossil data only indicate variation in salinity and stratification or are changes in trophic status also apparent? Availability of nutrients, seasonality and feeding strategies are also key factors to consider in controlling the dominance of one group over another. Chrysophyte cysts are traditionally used to indicate trophic status in lake systems [e.g., *Cronberg*, 1986; *Smol*, 1995]. *Smol* [1985], for example, suggested the ratio chrysophyte cysts to diatom valves (C/D) could be used to effectively trace past changes in length of growing season and lake trophic status (C/D ratio high = oligotrophy; C/D ratio low = eutrophy). If this method is applicable to the ACEX sediments, it brings into question whether the chrysophyte cysts represent algae producing seasonally in situ in central Arctic middle Eocene surface waters or were transported via river runoff from surrounding lacustrine deposits of the Arctic region. In the latter case, then there ought to be a correspondence between diatom abundance (the in situ bloomers responding quickly to river-borne nutrients) and chrysophyte cysts (the allochthons) as well as terrestrial geochemical proxies such as Fe/Al and Ti/Al. An intensified hydrological cycle in the warm Eocene meant that nutrient supply to the central Arctic likely came via a river-borne route whether chrysophytes were transported within it or not.

[35] Figure 7 shows relationships between Fe/Al, Ti/Al and chrysophyte cysts. The Fe/Al signal is high in the biosiliceous interval, compared with low values above 200 mcd and below 350 mcd [see *Expedition 302 Scientists*, 2006, for data] and is complicated by a high amount of

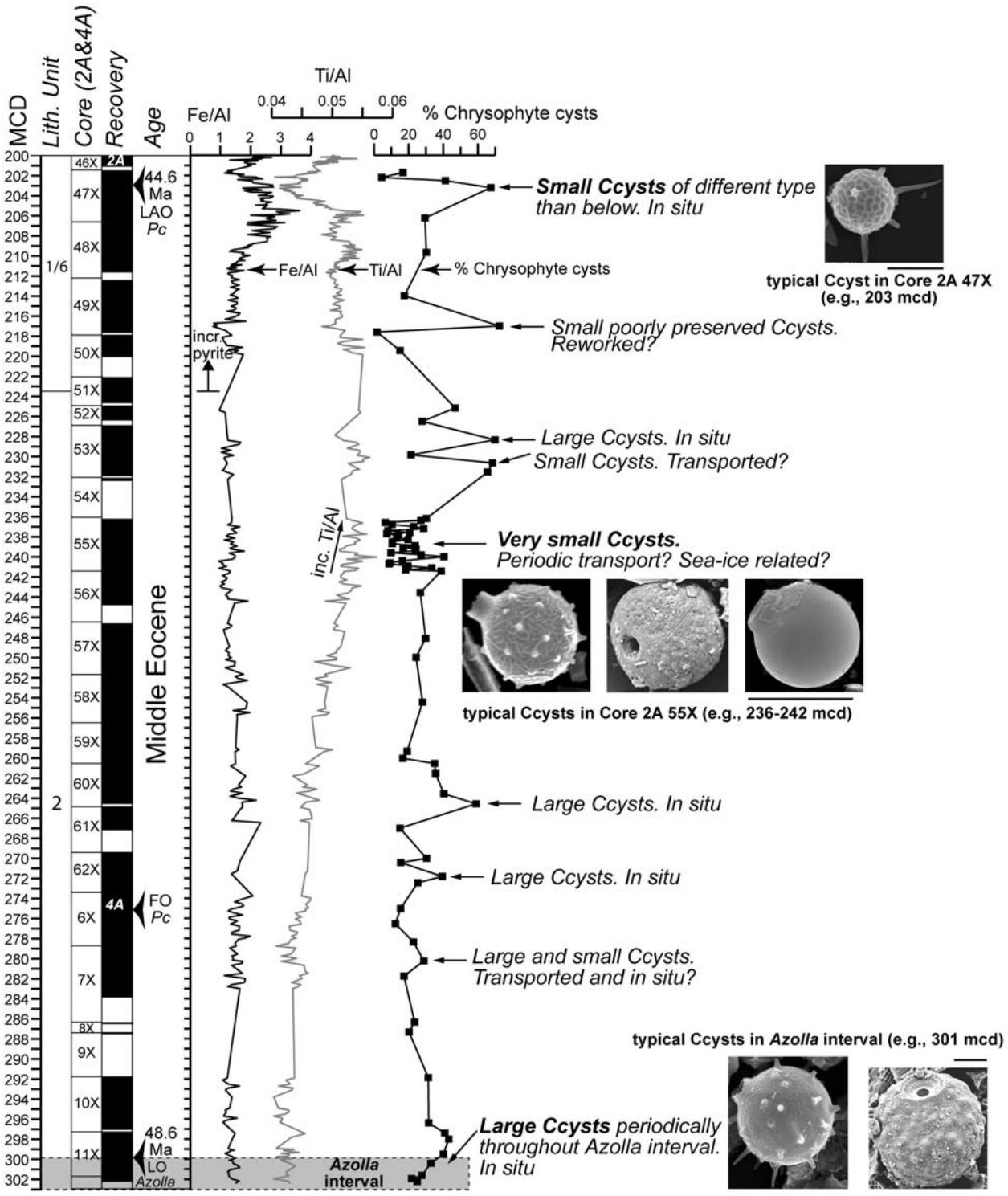

Figure 7. Relationships between the elemental ratios Fe/Al, Ti/Al, and chrysophyte cyst abundance. Images of six types of chrysophyte cyst are indicated against relevant text/core depth (scale bar = 5 μm).

pyrite, particularly in Subunit 1/6. For average shale the Fe/Al ratio is ~0.55 [*Wedepohl*, 1971]. Since values in the biosiliceous interval always greatly exceed 0.55 and humic matter-rich boreal river water is the most likely source for the excess in Fe, Fe/Al is good overall indication of significant riverine input for these sediments. Fe would have been easily trapped in this anoxic/euxinic environment with hydrogen sulfide as a trapping agent. Ti/Al, on the other hand, reflects either provenance or energy changes, e.g., an indicator of proximity to the paleoshoreline/clastic input and perhaps water depth. A change in provenance and/or energy is invoked for the large overall

difference in Ti/Al values between Unit 2 (above the *Azolla* interval) and Subunit 1/6.

[36] We suggest the majority of ACEX chrysophyte cysts reflect in situ production in the surface waters of the central Arctic under periodically stratified conditions. Several points of evidence bring us to this assumption: (1) chrysophyte cysts are very abundant throughout the biosiliceous interval (Figure 3b), which does not suggest overall mass transportation; (2) the relationship between chrysophyte cyst abundance, riverine input (Fe/Al), and energy changes (Ti/Al) is not obvious, although there is some covariance for short intervals; (3) there is generally no correspondence between diatom and chrysophyte cyst abundance (Figure 5b), suggesting in situ seasonal and trophic differences; (4) they are associated with high abundances of presumed in situ freshwater algae and freshwater tolerant dinocysts [e.g., *Expedition 302 Scientists*, 2006] particularly for the *Azolla* interval [*Brinkhuis et al.*, 2006]; and (5) within the *Azolla* interval, chrysophyte cysts are large (>10 μm, often up to $\sim$20 μm diameter; Figure 7), often highly ornamented morphotypes in excellent to pristine preservation, i.e., long delicate spines still intact suggesting minimal transportation. Following an assumed influx of warm salty water which brought about the eventual demise of *Azolla* in the region [*Brinkhuis et al.*, 2006], fresh surface waters that later returned to the central Arctic (e.g., 47.15 Ma; Figure 6) again supported chrysophytes which produced cyst morphotypes identical to those preserved within the *Azolla* interval.

[37] In situ chrysophyte production seems reasonable in light of the Arctic Ocean being still largely unconnected to the world's oceans at this time, i.e., a seasonally stable ''lake-type'' environment in the upper water layers. A modern analogue is the Baltic Sea where living freshwater chrysophytes are observed in the plankton of the Gulf of Finland and Southern Baltic proper [*Hällfors*, 2004]. Our hypothesis suggests shallow enough water depths (or halocline) to allow excystment (germination) consistent with a high proportion of diatom resting spores. An alternative scenario would be periodic river transportation of living chrysophyte algae from highly proximal terrestrial sources into the surface Arctic Ocean where they underwent encystment in situ. Either, or a combination of both hypotheses does not affect our estimation of relative salinity and stratification.

[38] Interestingly, in some short intervals when smaller or mixed size cysts are prominent, Ti/Al is higher, i.e., provenance changes allowing both in situ growth plus allochthonous transportation of small cysts. We assume in a runoff scenario for small chrysophyte cysts, that they were available for transportation at their point of origin. For example, in core 2A 55X [see also *Sangiorgi et al.*, 2008a] although relative chrysophyte cyst abundance is reduced (Figure 7), we cannot rule out the possibility that some cysts may be either (1) saline tolerant types, (2) types adapted to different (?cooler) temperatures than those in other intervals, (3) associated with sea ice at this time [e.g., *Moran et al.*, 2006; *St. John*, 2008], or (4) have been transported from lacustrine lakes. In all these instances the cysts are small (<10 μm, typically 2–5 μm diameter), often sparsely, or less delicately ornamented or smooth-walled (Figure 7). Similar simple smooth-walled morphotypes are preserved in middle Eocene lacustrine sediments from a kimberlite diatreme in the Canadian Northwest Territories (A. Wolfe, personal communication, 2007). Although our preliminary investigations show very general connections between cyst size and environmental parameters, clearly there is potential to refine these relationships for the ACEX sediments.

[39] Given that both the diatoms and the majority of chrysophytes were produced in situ in the central Arctic, and taking the C/D ratio of *Smol* [1985], if the upper water layers are considered as a normal lake, one solution might be to invoke eutrophic conditions when diatoms dominated and oligotrophic conditions when chrysophyte cysts dominated. This rather simplified view may not be applicable to the ACEX sediments for two reasons: (1) chrysophytes and diatoms were probably living above and below the halocline, respectively (i.e., at different water depths), and (2) nitrogen isotope data by *Knies et al.* [2008] show only moderately productive waters (low N:P ratio) existed for much of the time. Nonetheless, there may be seasonal changes in trophic status which cannot be distinguished by bulk sediment sample analysis. Careful examination of the laminations may give further insight into paleoecology and seasonality.

6.3. Paleoecology and Seasonality

[40] The biosiliceous ACEX sediments are laminated at millimeter to submillimeter scale. Light- and dark-colored laminations are apparent, although some are not contiguous (A. E. S. Kemp, personal communication, 2007). Figure 8 illustrates preliminary investigations into the content of some of the light-colored laminations in Unit 2 above the *Azolla* interval. In our example from core 2A 55X, the lamination is near-pure biosilica (confirmed by initial scanning electron microscope (SEM) analysis), comprising an assemblage dominated by just two diatoms: *Anaulus arcticus* and *Stephanopyxis* sp. Light-colored laminations in other parts of Unit 2 comprise nearly pure *Hemiaulus* spp. Some of the dark laminations (not shown) comprise mixed silicofossils, organic material and clays. Clearly detailed SEM work is required to confirm our findings, identify likely sublaminations and any long-term species successions. However, we speculate the laminations may be seasonally related and suggest that some of the light-colored laminations comprising just 1 or 2 diatom

Figure 8. Example of the contents of a single light-colored lamination in Unit 2, e.g., core 2A-55X-5, 30–42 cm (241–242.12 meters composite depth (mcd)). Core photo is indicated at left. Main figure is the view through a light microscope, at magnification $\times$500, of unprocessed (i.e., raw) light-colored sediment. Image shows near-pure biosilica comprising mostly two diatoms: *Anaulus arcticus* (segmented structures) and *Stephanopyxis* sp. (mesh-like structures). There are also less abundant *Hemiaulus* sp., ebridians, and silicoflagellates in this image and notably very little to virtually no organic or clastic material.

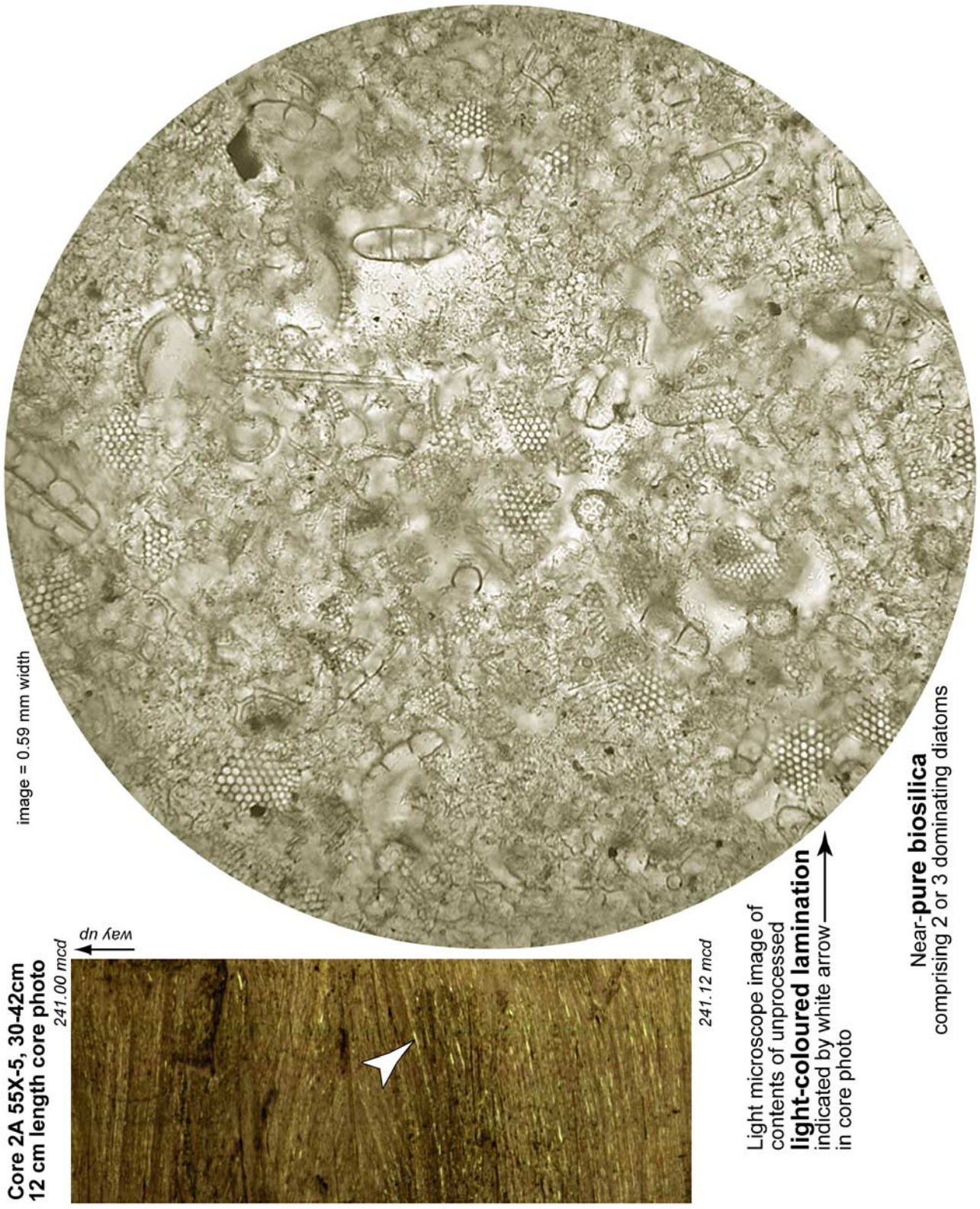
Core 2A 55X-5, 30-42cm
12 cm length core photo
241.00 mcd
241.12 mcd
up way
image = 0.59 mm width
Light microscope image of contents of unprocessed light-coloured lamination indicated by white arrow in core photo
Near-pure biosilica comprising 2 or 3 dominating diatoms

Figure 8

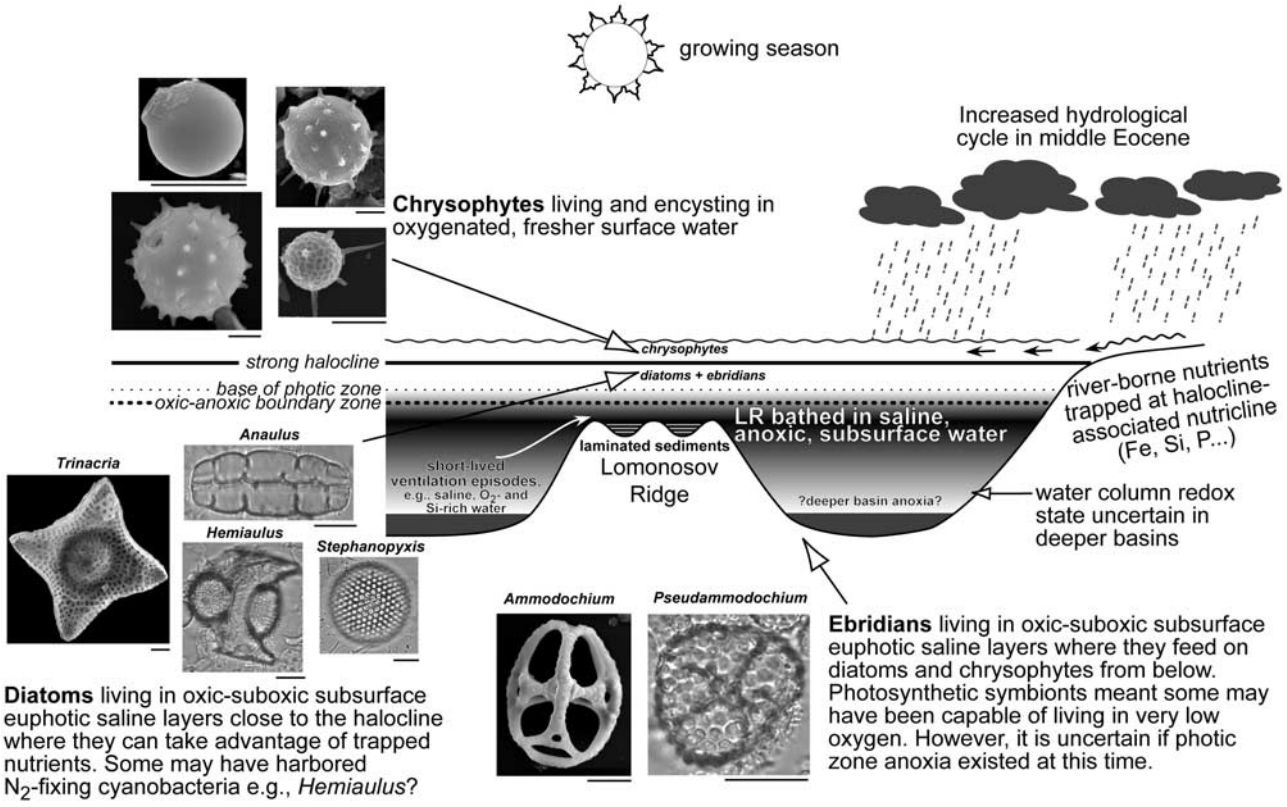

Figure 9. Environmental model of the central Arctic at the Lomonosov Ridge (LR) during the early middle Eocene, after the *Azolla* phase. Model represents polar daylight months (growing season) and is drawn as if looking from the Siberian margin toward Greenland. We envisage the LR as a submerged topographic high with variable topography, bathed in saline, anoxic water in which laminated sediments accumulated. Redox state of the deeper basins is unknown, particularly on the Canadian side as represented by the basin drawn to the right of the LR. Short-lived ventilation episodes via the Norwegian-Greenland Sea/North Atlantic are represented by the white arrow to the left of the LR. Scale bar = 5 μm for chrysophyte cysts and 10 μm for other images.

species represent bloom events. Increased seasonality in higher latitudes may have been an important parameter during the long Eocene cooling trend [*Zachos et al.*, 2001], and at this unusual location the growing season would have consisted of 6 months continuous daylight. Strong diatom seasonality is also suggested from the Alpha Ridge in laminated sediments of Late Cretaceous age [e.g., *Barron*, 1985; *Davies*, 2006] and middle Eocene age involving *Anaulus* [*Dell'Agnese and Clark*, 1994].

[41] We suggest Fe may have been the key factor in promoting seasonal diatom blooms for some species. As an important biolimiting nutrient [e.g., *Coale et al.*, 1996; *Boyd et al.*, 2000], diatom production is greatly catalyzed by Fe, even when other nutrients are abundant (e.g., the "high-nutrient, low-chlorophyll" regime of, e.g., the Southern Ocean). Fe availability also controls the degree of silicification [e.g., *Hutchins and Bruland*, 1998]. A rich supply of Fe reduces the silicic acid:nitrate uptake ratio in diatoms, resulting in thinner frustules [*Boyle*, 1998], the potential for differential dissolution and possible overestimation of robust (heavily silicified) diatoms in the sediments. However, both robust and more thinly silicified diatoms are preserved in the ACEX sediments so this does not appear to be an issue. The light-colored laminations dominated by *Anaulus arcticus* and *Stephanopyxis* sp. may represent blooms at the very start of the growing season (spring or early summer), following eutrophication by winter mixing, a return to sufficient light levels, but ultimately triggered by renewed Fe input. Since stratification is likely to have been developing during the early part of the growing season and the halocline was still relatively shallow, the diatoms were probably able to quickly exploit nutrients trapped relatively shallowly in the subsurface, more saline euphotic zone (Figure 9). In an analogy to the short-lived intensity of modern diatom blooms (a few days to weeks), competitors would have been precluded/overwhelmed during this time and subsequent flux to the seafloor would have been high enough to dilute other sedimentary signals. In this scenario, rapid flux must have occurred before the halocline was fully developed.

[42] In the case of light-colored laminations dominated by *Hemiaulus* spp. this "boom and bust" interpretation may not be appropriate if we take the analogy of the modern diatom *Hemiaulus hauckii*, known to be adapted to stratified, oligotrophic (N-limiting) conditions. This species forms near-monospecific sublaminations in Mediterranean Eemian sapropels [e.g., *Kemp et al.*, 1999]. Here it is inter-

preted as having generated considerable production in a deep chlorophyll maximum over several summer months, followed by rapid sedimentation after autumn/winter mixing (i.e., a "Fall dump") [*Kemp et al.*, 2000]. Low N:P estimates lead *Knies et al.* [2008] to suggest that N_2-fixing organisms existed over the LR. Biological N_2-fixation is an important source of N for supporting oceanic primary production and some diatoms such as *H. hauckii*, are known to be capable of this by harboring N_2-fixing cyanobacteria [e.g., *Villareal*, 1991; *Carpenter et al.*, 1999]. *Knies et al.* [2008] suggest the consistently high abundance of *Hemiaulus* spp. in the ACEX sediments (we estimate here up to 60% of the diatom assemblages in Unit 2) may be due to its ability to also harbor N_2-fixing cyanobacteria. However, not all the ACEX diatoms may have had this ability and some caution must be taken in placing too much emphasis on using modern species to interpret extinct assemblages where no analogy may exist. Also we don't know if the fossil ACEX species were adapted in the same way as modern species to the extremes of polar insolation. Nonetheless, a "Fall-dump" flux has been suggested for *Stephanopyxis palmeriana*-rich laminations in Gulf of California Holocene sediments [see *Kemp et al.*, 2000, and references therein] and for *Anaulus sibericus*-rich laminations in Alpha Ridge Late Cretaceous sediments [*Davies*, 2006]. Hence further work is clearly needed to refine these ideas for the ACEX setting, particularly in terms of which species (resting spores or vegetative cells) are involved, the seasonality and paleoecology of *Anaulus* in particular, relationships with Fe influx, the timing of specific blooms and their export flux and whether silicofossils other than diatoms form light-colored laminations.

[43] Regardless of which season is represented by diatom-dominated light-colored laminations, we suggest the dark-colored laminations represent the main part of the growing season (late spring or summer) after the initial spring diatom bloom (if any) as passed, when stratification is more developed, nutrients (particularly Fe and P) have been depleted somewhat and predators (e.g., ebridians and dinoflagellates) can take hold. We base this assumption on the mixed nature of these laminations but recognize detailed SEM work is required. Hence the dark-colored laminations may represent "normal" background sedimentation while the light-colored laminations represent rapid flux dilution episodes.

[44] *Onodera et al.* [2008, and references therein] show that modern ebridians can survive in suboxic waters by harboring symbiotic photosynthetic bacteria and suggest this is likely the case for the ACEX fauna. The ebridians therefore may have thrived in the lower, euphotic, saline layer, beneath the strong halocline (Figure 9). Chrysophytes are fierce competitors in harsh environments (i.e., oligotrophic P-limiting, cold temperatures), which may in part reflect their diverse nutritional strategies [e.g., *Zeeb and Smol*, 2001, and references therein]. We suggest they bloomed and underwent encystment after the initial diatom bloom in the uppermost low-salinity surface waters (Figure 9) once nutrients, particularly P, were limiting. Ebridians may have fed on living chrysophytes, other freshwater algae and freshwater tolerant dinoflagellates from just below the stratified layer and on diatoms and marine dinoflagellates in the same subsurface layer.

7. Summary and Conclusions

[45] New siliceous microfossil data from sediment cores recovered by ACEX drilling on the Lomonosov Ridge are presented. These cores represent the first long-core recovery of Paleogene sediments from the Arctic. Our study provides some of the first insights into central Arctic paleoenvironments spanning a ~5 Ma interval of the middle Eocene, at the start of the global transition from greenhouse to icehouse conditions. Changes in the dominance of diatoms, chrysophyte cysts and ebridians, indicate relative salinity, stratification and nutrient changes. During the growing season we envisage a stratified water column with a strong halocline and anoxia at depth. Above the halocline, chrysophytes bloomed and underwent encystment in the uppermost, fresher layers. Below the halocline, ebridians and diatoms, adapted in different ways to stratification, survived in the more saline euphotic layers. This model accounts for the cooccurrence of freshwater and brackish to marine siliceous microfossils. Superimposed on this model were times when diatoms were dominant, notably ~48.1 to ~47.5 Ma and ~47 to ~46 Ma. We interpret these as phases of increased salinity, weaker stratification (shallower halocline) and more mixed conditions. Chrysophytes dominated during the *Azolla* phase, ~47.5 to ~47 Ma and ~44.6 Ma. We interpret these as times of reduced salinity, stronger stratification (deeper halocline) and more stable conditions. Salinity fluctuations were likely controlled by precipitation and river input but further work is needed to identify sea level changes. Laminations may record seasonal changes which help constrain this model further.

[46] **Acknowledgments.** This research used samples provided by the Integrated Ocean Drilling Program (IODP). CES and NK acknowledge VISTA (Norwegian Academy of Science and Letters and Statoil) Project 6248 and the Research Council of Norway (RCN). Extended thanks go to Alex Wolfe for invaluable discussions on chrysophytes and their cysts, and also to Jonaotaro Onodera for data and help in understanding ebridian ecology and their interpretation in the ACEX cores. Thanks to John Barron for informative discussions on fossil Arctic/Northern Hemisphere diatoms, and to Steve Bohaty, an anonymous reviewer, and Martin Pearce for helpful suggestions for improvements to an earlier draft of this manuscript. We also acknowledge the following for useful ACEX discussions: J. Backman, K. Katsuki, K. Takahashi, T. Moore, L. Waddelin, J. Knies, K. St. John, F. Sangiorgi, H. Brinkhuis, A. Sluijs, M. O'Regan, A. Davies, and A.E.S. Kemp.

References

Adam, D. P., and A. D. Mahood (1981), Chrysophyte cysts as potential environmental indicators, *Geol. Soc. Am. Bull., Part 1*, *92*, 839–844.

Backman, J., et al. (2008), Age model and core-seismic integration for the Cenozoic Arctic Coring Expedition sediments from the Lomonosov Ridge, *Paleoceanography*, doi:10.1029/2007PA001476, in press.

Barron, J. A. (1985), Diatom biostratigraphy of the CESAR 6 core, Alpha Ridge, in *Initial Geological Report on Cesar: The Canadian Expedition to Study the Alpha Ridge, Arctic Ocean*, edited by H. R. Jackson et al., *Pap. Geol. Surv. Can.*, *84–22*, 137–148.

Barron, J. A., D. Bukry, and R. Z. Poore (1984), Correlation of the middle Eocene Kellogg Shale of northern California, *Micropaleontology*, *30*, 138–170.

Battarbee, R. W., and M. J. Kneen (1982), The use of electronically counted microspheres in absolute diatom analysis, *Limnol. Oceanogr.*, *27*, 184–188.

Bohaty, S. M., and D. M. Harwood (2000), Ebridian and silicoflagellate biostratigraphy from Eocene McMurdo erratics and the Southern Ocean, in *Paleobiology and Paleoenvironments of Eocene Rocks, McMurdo Sound, East Antarctica*, *Ant. Res. Ser.*, vol. 76, edited by J. D. Stillwell and R. M. Feldmann, pp. 99–159, AGU, Washington, D. C.

Boyd, P., et al. (2000), A mesoscale phytoplankton bloom in the polar Southern Ocean stimulated by iron fertilization, *Nature*, *407*, 695–702, doi:10.1038/35037500.

Boyle, E. (1998), Pumping iron makes thinner diatoms, *Nature*, *393*, 733–744, doi:10.1038/31585.

Brinkhuis, H., et al. (2006), Episodic fresh surface waters in the early Eocene Arctic Ocean, *Nature*, *441*, 606–609, doi:10.1038/nature04692.

Brumsack, H.-J. (2006), The trace metal content of recent organic carbon-rich sediments: Implications for Cretaceous black shale formation, *Palaeogeogr. Palaeoclimatol. Palaeoecol.*, *232*, 344–361.

Brumsack, H.-J., F. Sangiorgi, H. Brinkhuis, R. Stein, and B. Schnetger (2007), Paleogene black shales from the central Arctic Ocean, *Geophys. Res. Abs.*, *9* (10272), Eur. Geosci. Union, Vienna, April.

Bukry, D. (1984), Paleogene paleoceanography of the Arctic Ocean is constrained by the middle or late Eocene age of the USGS core Fl-4 501 22; evidence from silicoflagellates, *Geology*, *12*, 199–201.

Bukry, D. (1985), Correlation of Late Cretaceous Arctic silicoflagellates from Alpha Ridge, *Pap. Geol. Surv. Can.*, *84–22*, 125–135.

Carpenter, E. J., J. P. Montoya, J. Burns, M. R. Mulholland, A. Subramaniam, and D. G. Capone (1999), Extensive bloom of a N2 fixing diatom/cyanobacterial association in the tropical Atlantic Ocean, *Mar. Ecol. Prog. Ser.*, *185*, 273–283.

Coale, K., et al. (1996), A massive phytoplankton bloom induced by an ecosystem-scale iron fertilization experiment in the equatorial Pacific Ocean, *Nature*, *383*, 495–501, doi:10.1038/383495a0.

Cornell, W. C. (1972), Late Cretaceous chrysomonad cysts, *Palaeogeogr. Palaeoclimatol. Palaeoecol.*, *12*, 33–47.

Cronberg, G. (1986), Chrysophycean cysts and scales in lake sediments: A review, in *Chrysophytes: Aspects and Problems*, edited by J. Kristiansen and R. A. Andersen, pp. 281–315, Cambridge Univ. Press, Cambridge.

Davies, A. (2006), High resolution palaeoceanography and palaeoclimatology from mid and high latitude Late Cretaceous laminated sediments, unpub. Ph.D. thesis, Univ. of Southampton, Faculty of Eng., Sci. and Math., School of Ocean and Earth Sci., Southampton, UK.

Dell'Agnese, D., and D. L. Clark (1994), Siliceous microfossils from the warm Late Cretaceous and early Cenozoic Arctic Ocean, *J. Paleontol.*, *68*, 31–46.

Duff, K. E., B. A. Zeeb, and J. P. Smol (1994), *Atlas of Chrysophycean Cysts Volume 1, Developments in Hydrobiology*, vol. 99, 189 pp., Kluwer Acad., Dordrecht, Netherlands.

Dzinoridze, R. N., A. P. Jousé, G. S. Koroleva-Golikova, G. E. Kozlova, G. S. Nagaeva, M. G. Petrushevskaya, and N. I. Strelnikova (1978), Diatom and radiolarian Cenozoic stratigraphy, Norwegian Basin: DSDP Leg 38, in *Initial Reports of the Deep Sea Drilling Project; Supplement to Volumes 38, 39, 40, and 41*, edited by S. M. White et al., pp. 289–427, Texas A & M Univ., Ocean Drill. Program, College Station, Tex.

Edlund, M. B., and E. F. Stoermer (2000), A 200,000-year, high-resolution record of diatom productivity and community makeup from Lake Baikal shows high correspondence to the marine oxygen-isotope record of climate change, *Limnol. Oceanogr.*, *45*, 948–962.

Eldrett, J. S., I. C. Harding, J. V. Firth, and A. P. Roberts (2004), Magnetostratigraphic calibration of Eocene–Oligocene dinoflagellate cyst biostratigraphy from the Norwegian-Greenland Sea, *Mar. Geol.*, *204*, 91–127.

Ernisse, J., and K. McCartney (1993), Ebridians, in *Fossil Prokaryotes and Protists*, edited by J. H. Lipps, pp. 131–140, Blackwell Sci., Boston.

Expedition 302 Scientists (2006), Sites M0001–M0004, in *Arctic Coring Expedition (ACEX)*, *Proc. Integr. Ocean Drill. Program*, *302*, doi:10.2204/iodp.proc.302.104.2006.

Fenner, J. (1985), Late Cretaceous to Oligocene planktic diatoms, in *Plankton Stratigraphy*, edited by H. M. Bolli et al., pp. 713–762, Cambridge Univ. Press.

Fenner, J. (1994), Diatoms of the Für Formation, their taxonomy and biostratigraphic interpretation: Results from the Harre borehole, Denmark, *Aarhus Geosci.*, *1*, 99–163.

Gleser, Z. I. (1994), Correlation of development stages of the Paleogene diatom flora from marine epicontinental and oceanic basins, *Stratigr. Geol. Correl.*, *2*, 95–98.

Gleser, Z. I. (1996), Problems of Eocene siliceous phytoplankton zonation (exemplified by the Caspian Eocene deposits), *Stratigr. Geol. Correl.*, *4*, 392–402.

Gombos, A. M., Jr. (1977), Archaeomonads as Eocene and Oligocene guide fossils in marine sediments, *Initial Rep. Deep Sea Drill. Proj.*, *36*, 689–695.

Gombos, A. M., Jr. (1982), Early and middle Eocene diatom evolutionary events, *Bacillaria*, *5, 225–242.*

Gombos, A. M., Jr. (1987), Middle Eocene diatoms from the North Atlantic, Deep Sea Drilling Project 605, *Initial Rep. Deep Sea Drill. Proj.*, *93*, 793–799.

Hajós, M. (1976), Upper Eocene and lower Oligocene Diatomaceae, Archaeomonadaceae, and Silicoflagellatae in southwestern Pacific sediments, DSDP Leg 29, in *Initial Reports of the DSDP*, *35*, 817–883.

Hällfors, G. (2004), Checklist of Baltic Sea phytoplankton species (including some heterotrophic protistan groups), in *Baltic Sea Environment Proceedings*, vol. 95, 210 pp., Helsinki Comm., Baltic Mar. Environ. Comm., Helsinki.

Hargraves, P. E. (2002), The ebridian flagellates *Ebria* and *Hermesinum*, *Plankton Biol. Ecol.*, *49*, 9–16.

Harwood, D. M., and R. Gersonde (1990), Lower Cretaceous diatoms from ODP Leg 113 Site 693 (Weddell Sea). part 2: Resting spores, chrysophycean cysts, an endoskeletal dinoflagellate, and notes on the origin of diatoms, *Proc. Ocean Drill. Progr. Sci. Results*, *113*, 403–425.

Harwood, D. M., and V. A. Nikolaev (1995), Cretaceous diatoms: Morphology, taxonomy, biostratigraphy, in *Short Courses in Paleontology*, vol. 8, *Siliceous Microfossils*, edited by C. D. Blome et al., pp. 81–106, Paleontol. Soc., Tulsa, Okla.

Hendey, N. I., and P. A. Sims (1984), Some new or unusual Eocene Biddulphioid diatoms, *I. Bacillaria*, *7*, 59–90.

Hewson, I., J. M. O'Neil, and E. Abal (2001), A low-latitude bloom of the surf-zone diatom, *Anaulus australis* (Centrales, Bacillariophyta) on the coast of Southern Queensland (Australia), *J. Plankton Res.*, *23*, 1233–1236.

Hibberd, D. J. (1977), Ultrastructure of cysts formation in *Ochromonas tuberculata* (Chrysophyceae), *J. Phycol.*, *13*, 309–320.

Homann, M. (1991), Die Diatomeen der Für-Formation (Alttertiär, Limfjord/Dänemark, *Geol. Jahrb. Reihe A*, *123*, 1–285.

Hoppenrath, M., and B. S. Leander (2006), Ebriid Phylogeny and the Expansion of the Cercozoa, *Protist*, *157*, 279–290.

Huckriede, H., and D. Meischner (1996), Origin and environment of manganese-rich sediments within black-shale basins, *Geochim. Cosmochim. Acta*, *60*, 1399–1413.

Hutchins, D. A., and K. W. Bruland (1998), Iron-limited diatom growth and Si:N uptake ratios in a coastal upwelling regime, *Nature*, *393*, 561–564, doi:10.1038/31203.

Jahren, A. H., and L. S. L. Sternberg (2002), Eocene meridional weather patterns reflected in the oxygen isotopes of Arctic fossil wood, *GSA Today*, 4–9, January.

Jahren, A. H., and L. S. L. Sternberg (2003), Humidity estimate for the middle Eocene Arctic rain forest, *Geology*, *31*, 463–466.

Jakobsson, M., et al. (2007), The early Miocene onset of a ventilated circulation regime in the Arctic Ocean, *Nature*, *447*, 986–990, doi:10.1038/nature05924.

Jenkyns, H. C., A. Forster, S. Schouten, and J. S. Sinninghe Damsté (2004), High temperatures in the Late Cretaceous Arctic Ocean, *Nature*, *432*, 888–892, doi:10.1038/nature03143.

Kanaya, T. (1957), Eocene diatom assemblages from the Kellogg and "Sidney" Shales, Mt. Diablo area, California, *Sci. Rep. Tohoku Univ., Ser. 2*, *28*, 27–124.

Kemp, A. E. S., R. B. Pearce, I. Koizumi, J. Pike, and S. J. Rance (1999), The role of mat-forming diatoms in the formation of Mediterranean sapropels, *Nature*, *398*, 57–61, doi:10.1038/18001.

Kemp, A. E. S., J. Pike, R. B. Pearce, and C. B. Lange (2000), The 'Fall dump': A new perspective on the role of a 'shade flora' in the annual cycle of diatom production and export flux, *Deep Sea Res., Part II*, *47*, 2129–2154.

Knies, J., U. Mann, B. Popp, R. Stein, and H.-J. Brumsack (2008), Surface water productivity and paleoceanographic implications in the Cenozoic Arctic Ocean, *Paleoceanography*, doi:10.1029/2007PA001455, in press.

Konovalov, S. K., and J. W. Murray (2001), Variations in the chemistry of the Black Sea on a time scale of decades (1960–1995), *J. Mar. Syst.*, *31*, 217–243.

Lipps, J. H., and K. McCartney (1993), Chrysophytes, in *Fossil Prokaryotes and Protists*, edited by J. H. Lipps, pp. 141–154, Blackwell Sci., Boston.

Lyons, T. W., and S. Severmann (2006), A critical look at iron paleoredox proxies: New insights from modern euxinic marine basins, *Geochim. Cosmochim. Acta*, *70*, 5698–5722.

McGowran, B. (1989), Silica burp in the Eocene ocean, *Geology*, *17*, 857–860.

Miller, K. G., J. D. Wright, and J. V. Browning (2005), Visions of ice sheets in a greenhouse world, *Mar. Geol.*, *217*, 215–231.

Moran, K., et al. (2006), The Cenozoic palaeoenvironment of the Arctic Ocean, *Nature*, *441*, 601–605, doi:10.1038/nature04800.

Nicholls, K. H., and D. E. Wujek (2003), Chrysophycean Algae, in *Freshwater Algae of North America: Ecology and Classification*, edited by J. D. Wehr and R. G. Sheath, pp. 471–509, Academic, New York.

Onodera, J., K. Takahashi, and R. W. Jordan (2008), Eocene silicoflagellate and ebridian paleoceanography in the central Arctic Ocean, *Paleoceanography*, *23*, PA1S15, doi:10.1029/2007PA001474.

O'Regan, M., et al. (2008), Mid-Cenozoic tectonic and paleoenvironmental setting of the central Arctic Ocean, *Paleoceanography*, doi:10.1029/2007PA001559, in press.

Oreshkina, T. V., G. N. Aleksandrova, and G. E. Kozlova (2004), Early Eocene marine planktonic record of the East Urals margin (Sverdlovsk region): Biostratigraphy and paleoenvironments, *Neues Jahrb. Geol. Palaeontol. Abh.*, *234*, 201–222.

Osawa, M., K. Takahashi, and B. J. Hay (2005), Shell-bearing plankton fluxes in the central Black sea, 1989–1991, *Deep Sea Res., Part I*, *52*, 1677–1698.

Perch-Nielsen, K. (1975), Late Cretaceous to Pleistocene archaeomonads, ebridians, endoskeletal dinoflagellates, and other siliceous microfossils from the subantarctic southwest Pacific, DSDP, Leg 29, *Initial Rep. Deep Sea Drill. Proj.*, *29*, 873–907.

Radionova, E. P., and I. E. Khokhlova (2000), Was the North Atlantic connected with the Tethys via the Arctic in the early Eocene? Evidence from siliceous plankton, in *Early Paleogene Warm Climates and Biosphere Dynamics: Short Papers and Extended Abstracts*, edited by B. Schmitz, B. Sundquist, and F. P. Andreasson, *GFF*, *122*(1), 133–134.

Radionova, E. P., T. V. Oreshkina, I. E. Khokhlova, and V. N. Ben'yamovskii (1994), Eocene deposits on the northeastern slope of the Dneiper-Donets Depression: Zonal stratigraphy and cyclic analysis, *Stratigr. Geol. Correl.*, *2*, 563–580.

Radionova, E. P., V. N. Beniamovski, A. I. Iakovleva, N. G. Muzylöv, T. V. Oreshkina, E. A. Shcherbinina, and G. E. Kozlova (2003), Early Paleogene transgressions: Stratigraphical and sedimentological evidence from the northern Peri-Tethys, in *Causes and Consequences of Globally Warm Climates in the Early Paleogene*, edited by S. L. Wing et al., pp. 239–261, *Geol. Soc. of Am., Spec. Pap.*, *393*, Boulder, Colo.

Sangiorgi, F., E. E. van Soelen, D. J. A. Spofforth, H. Pälike, C. E. Stickley, K. St. John, N. Koç, S. Schouten, J. S. Sinninghe Damsté, and H. Brinkhuis (2008a), Cyclicity in the middle Eocene central Arctic Ocean sediment record: Orbital forcing and environmental response, *Paleoceanography*, doi:10.1029/2007PA001487, in press.

Sangiorgi, F., H.-J. Brumsack, D. A. Willard, S. Schouten, C. E. Stickley, M. O'Regan, G.-J. Reichart, J.-S. Sinninghe Damsté, and H. Brinkhuis (2008b), A 26 million years gap in the central Arctic record at the greenhouse-icehouse transition: Looking for clues, *Paleoceanography*, *23*, PA1S04, doi:10.1029/2007PA001477.

Scherer, R., and N. Koç (1996), Late Paleogene diatom biostratigraphy and paleoenvironments of the northern Norwegian-Greenland Sea, *Proc. Ocean Drill. Program Sci. Results*, *151*, 75–99.

Schrader, H. J., and J. Fenner (1976), Norwegian Sea Cenozoic diatom biostratigraphy and taxonomy, *Initial Rep. Deep Sea Drill. Proj.*, *38*, 921–1099.

Siver, P. A., and A. P. Wolfe (2005a), Eocene scaled chrysophytes with pronounced modern affinities, *Int. J. Plant Sci.*, *166*, 533–536.

Siver, P. A., and A. P. Wolfe (2005b), Scaled chrysophytes in middle Eocene lake sediments from northwestern Canada, including descriptions of six new species, *Nova Hedwigia Beihefte*, *128*, 295–308.

Siver, P. A., and A. P. Wolfe (2007), *Eunotia* spp. (Bacillariophyceae) from middle Eocene lake sediments and comments on the origin of the diatom raphe, *Can. J. Bot.*, *85*, 83–90.

Skogstad, A., and O. L. Reymond (1989), An ultrastructural study of vegetative cells, encystment, and mature statospores, in *Spiniferomonas bourrellyi* (Chrysophyceae), *Beiheft Nova Hedwigia*, *95*, 71–79.

Sluijs, A., et al. (2006), Subtropical Arctic Ocean temperatures during the Palaeocene Eocene thermal maximum, *Nature*, *441*, 610–613, doi:10.1038/nature04668.

Smol, J. P. (1985), The ratio of diatom frustules to chrysophycean statospores: A useful paleolimnological index, *Hydrobiologia*, *123*, 199–208.

Smol, J. P. (1988), Chrysophycean microfossils in paleolimnological studies, *Palaeogeogr. Palaeoclim. Palaeoecol.*, *62*, 287–297.

Smol, J. P. (1995), Application of chrysophytes to problems in paleoecology, in *Chrysophyte algae: Ecology, Phylogeny and Development*, edited by C. Sandgren et al., pp. 303–329, Cambridge Univ. Press.

Stein, R., B. Boucsein, and H. Meyer (2006), Anoxia and high primary production in the Paleogene central Arctic Ocean: First detailed records from Lomonosov Ridge, *Geophys. Res. Lett.*, *33*, L18606, doi:10.1029/2006GL026776.

St. John, K. E. (2008), Cenozoic ice-rafting history of the central Arctic Ocean: Terrigenous sands on the Lomonosov Ridge, *Paleoceanography*, *23*, PA1S05, doi:10.1029/2007PA001483.

Strelnikova, N. I. (Ed.) (2006), *Diatom Algae of Russia and Adjacent Countries, Fossil and Recent*, *2* (4), 180 pp., St. Petersburg Univ. Press.

Suto, I., R. W. Jordan, and M. Watanabe (2008a), Taxonomy of the fossil marine diatom resting spore genus *Goniothecium* Ehrenberg and its allied species, *Diatom Res.*, in press.

Suto, I., M. Watanabe, and R. W. Jordan (2008b), Taxonomy of the fossil marine diatom resting spore genus *Odontotropis* Grunow, *Diatom Res.*, in press.

Suto, I., R. W. Jordan, and M. Watanabe (2008c), Taxonomy of middle Eocene diatom resting spores and their allied taxa from IODP sites in the central Arctic Ocean (the Lomonosov Ridge), *Micropaleontology*, in press.

Talbot, M. M. B., and G. C. Bate (1986), Diel periodicities in cell characteristics of the surf-zone diatom *Anaulus birostratus*: Their role in the dynamics of cell patches, *Mar. Ecol. Prog. Ser.*, *32*, 81–89.

Tapia, P. M., and D. M. Harwood (2002), Upper Cretaceous diatom biostratigraphy of the Arctic Archipelago and northern continental margin, Canada, *Micropaleontology*, *48*, 303–342.

Villareal, T. A. (1991), Nitrogen-fixation by the cyanobacterial symbiont of the diatom genus *Hemiaulus*, *Mar. Ecol. Prog. Ser.*, *76*, 201–204.

Waddell, L. M., and T. C. Moore (2008), Salinity of the Eocene Arctic Ocean from oxygen isotope analysis of fish bone carbonate, *Paleoceanography*, doi:10.1029/2007PA001451, in press.

Wedepohl, K. H. (1971), Environmental influence on the chemical composition of shales and clays, in *Physics and Chemistry of the Earth*, vol. 8, edited by L. H. Ahrens et al., pp. 305–333, Pergamon, Oxford, UK.

Wilkinson, A. N., B. A. Zeeb, and J. P. Smol (2002), *Atlas of Chrysophycean Cysts: Volume II, Developments in Hydrobiology*, vol. 157, 160 pp., Kluwer Acad., Dordrecht, Netherlands.

Wolfe, A. P., and M. B. Edlund (2005), Taxonomy, phylogeny, and paleoecology of *Eoseira wilsonii* gen. et sp. nov., a middle Eocene diatom (Bacillariophyceae: Aulacoseiraceae) from Horsefly, British Columbia, Canada, *Can. J. Earth Sci.*, *42*, 243–257.

Wolfe, A. P., and B. B. Perren (2001), Chrysophyte microfossils record marked responses to recent environmental changes in high- and mid-Arctic lakes, *Can. J. Bot.*, *79*, 747–752.

Yool, A., and T. Tyrrell (2005), Implications for the history of Cenozoic opal deposition from a quantitative model, *Palaeogeogr. Palaeoclimatol. Palaeoecol.*, *218*, 239–255.

Zachos, J. C., M. Pagani, L. C. Sloan, E. Thomas, and K. Billups (2001), Trends, rhythms, and aberrations in global climate 65 Ma to present, *Science*, *292*, 686–693.

Zeeb, B. A., and J. P. Smol (2001), Chrysophyte scales and cysts, in *Tracking Environmental Change Using Lake Sediments. Developments in Paleoenvironmental Research*, vol. 3, *Terrestrial, Algal, and Siliceous Indicators*, edited by J. P. Smol et al., pp. 203–223, Kluwer Acad., Dordrecht, Netherlands.

H.-J. Brumsack, Institute for Chemistry and Biology of the Marine Environment (ICBM), Oldenburg University, P.O. Box 2503, D-26111 Oldenburg, Germany.

R. W. Jordan, Department of Earth and Environmental Sciences, Yamagata University, Yamagata 990-8560, Japan.

N. Koç and C. E. Stickley, Norwegian Polar Institute, Polar Environmental Centre, N-9296 Tromsø, Norway. (catherine.stickley@npolar.no)

I. Suto, Department of Earth and Planetary Sciences, Nagoya University, Chikusa, Nagoya 464-8601, Japan.